8-1-1960

The Scattering of a Plane Electromagnetic Wave by a Finite Cone

C. C. Rogers
Purdue University

F. V. Schultz
Purdue University

ERD-TN-60-765
AF 19(604)4051

PURDUE UNIVERSITY
SCHOOL OF ELECTRICAL ENGINEERING

The Scattering of a Plane Electromagnetic Wave by a Finite Cone

C. C. Rogers and F. V. Schultz

AUGUST 1960

PREPARED FOR
ELECTRONICS RESEARCH DIRECTORATE
AIR FORCE CAMBRIDGE RESEARCH LABORATORIES
AIR FORCE RESEARCH DIVISION
AIR RESEARCH AND DEVELOPMENT COMMAND
UNITED STATES AIR FORCE
BEDFORD, MASSACHUSETTS
BY
PURDUE RESEARCH FOUNDATION, LAFAYETTE, INDIANA

ERD-TN-60-765

THE SCATTERING OF A PLANE ELECTROMAGNETIC WAVE BY A FINITE CONE

C. C. Rogers and F. V. Schultz

Purdue Research Foundation
Lafayette, Indiana

Scientific Report No. 1

AF 19(604)4051

August 1, 1960

Prepared

for

ELECTRONICS RESEARCH DIRECTORATE
AIR FORCE CAMBRIDGE RESEARCH LABORATORIES
AIR FORCE RESEARCH DIVISION
AIR RESEARCH AND DEVELOPMENT COMMAND
UNITED STATES AIR FORCE
BEDFORD, MASSACHUSETTS

Requests for additional copies by Agencies of the Department of Defense, their contractors, and other Government agencies should be directed to the:

ARMED SERVICES TECHNICAL INFORMATION AGENCY
ARLINGTON HALL STATION
ARLINGTON 12, VIRGINIA

Department of Defense contractors must be established for ASTIA services or have their 'need-to-know' certified by the cognizant military agency of their project or contract.

All other persons and organizations should apply to the:

U. S. DEPARTMENT OF COMMERCE
OFFICE OF TECHNICAL SERVICES
WASHINGTON 25, D.C.

ACKNOWLEDGMENT

The authors are indebted to Prof. I. Marx of the Department of Mathematics and Mr. M. R. Halsey of the School of Electrical Engineering for their assistance in making this report possible.

The experimental data and prepublication manuscripts furnished by Mr. R. E. Hiatt of the Radiation Laboratory at the University of Michigan are also sincerely appreciated.

TABLE OF CONTENTS

LIST OF ILLUSTRATIONS

LIST OF TABLES

ABSTRACT

This paper treats the solution of the vector Helmholtz equation for the case of a plane electromagnetic wave at 'nose-on' incidence on a perfectly-conducting cone of finite size. The solution presented is exact and in the form of an infinite series of spherical harmonics. The expansion coefficients of the series are determined by a set of an infinite number of equations involving an infinite number of unknowns. A discussion and numerical investigation of the field singularities at the tip and edge of the cone are included, as well as graphs of the associated Legendre functions of non-integral degree, $P_{\upsilon}^{1}(\cos\theta)$, and their first derivatives.

GLOSSARY OF SYMBOLS

$z_\upsilon(x)$ — Any spherical Bessel function of order υ and argument x, $\sqrt{\pi/2x}\ Z_{\upsilon+\frac{1}{2}}(x)$

$j_\upsilon(x)$ — Spherical Bessel function of the first kind of order υ and argument x

$h_\upsilon(x)$ — Spherical Hankel function of the second kind of order υ and argument x, $j_\upsilon(x) - in_\upsilon(x)$.

$n_\upsilon(x)$ — Spherical Neumann function (Bessel function of the second kind) of order υ and argument x

$Z_\upsilon(x)$ — Cylindrical Bessel function of any kind

$z'_\upsilon(x)$ — $\frac{1}{x}\ \frac{d}{dx}\ [xz_\upsilon(x)]$

$P^m_\upsilon(\cos\ \theta)$ — Associated Legendre function of order m and degree υ.

$\Gamma(x)$ — Gamma function of argument x. If $x = n$, an integer, $\Gamma(n) = (n-1)!$

γ_n — Expansion coefficient in the vector expansion of the negative travelling plane wave, $\bar{a}_x e^{i(\omega t+kz)}$,

$$\gamma_n = i^n \frac{2n+1}{n(n+1)}$$

δ^n_m — Kronecker delta $= \begin{cases} 1, & m=n \\ 0, & m\neq n \end{cases}$

$\delta(\theta)$
$\epsilon(\theta)$ — Error functions

$\mathcal{J}_n$ — Expansion coefficient in the vector expansion of the negative travelling plane wave, $\bar{a}_x e^{i(\omega t+kz)}$,

$$\mathcal{J}_n = -i\gamma_n$$

ϵ_o — Permittivity of free space, $\frac{1}{36\pi} \times 10^{-9}$ farad/meter

η	Intrinsic impedance of free space, $\sqrt{\mu_o/\epsilon_o}$
θ	Angular variable in spherical coordinates measured from the positive z axis
λ	Wavelength
μ	Non-integral degree of the associated Legendre function and a root of the equation $P_\mu^1(\cos\theta_o) = 0$.
υ	Non-integral degree of the associated Legendre function and a root of the equation $\left.\frac{dP_\upsilon^1}{d\theta}\right\|_{\theta=\theta_o} = 0$
μ_o	Permeability of free space, $4\pi \times 10^{-7}$ henry/meter
ρ	Radial coordinate in cylindrical coordinates, or kr, where r is the radial spherical coordinate
$\sigma = \infty$	Infinite conductivity
σ	Total back-scattering radar cross section
τ	Any general degree of the associated Legendre function, $P_\tau^m(\cos\theta)$
ϕ	Angular variable in spherical coordinates measured from the x axis.
ω	Angular frequency
Φ	A solution of the scalar wave equation
m,n	Positive integer or zero
$\bar{A}$	A vector
$\bar{E}$	Electric field
$\bar{H}$	Magnetic field
$\bar{S}$	The average Poynting vector, $\frac{1}{2}\,\mathrm{Re}(\bar{E} \times \bar{H}^*)$
$\bar{a}_i$	Unit vector in the i^{th} direction
k	Propagation constant, $2\pi/\lambda$

ERRATA

Page	Line	Incorrect	Correct
iv	16	25	26
iv	17	Date	Data
1	12	Franz[3]	Franz[35]
1	23	parabaloid	paraboloid
15	1	(37) from (37)	(37) from (36)
15	10	$[\ _{n}j_{n}(kb)+d_{n}h_{n}(kb)]$	$[\ _{n}j_{n}'(kb)+d_{n}h_{n}'(kb)]$
18	2	$d_{m}h_{m}(kb)$	$d_{m}h_{m}'(kb)$
19	6	$\frac{dP_{m}^{1}}{d\theta}\Big\|_{\theta\ \theta_{o}}$	$\frac{dP_{m}^{1}}{d\theta}\Big\|_{\theta=\theta_{o}}$
19	6	$v(v+1)$	$\frac{v(v+1)}{m(m+1)}$
22	6	χ_{n}	$_{c}\chi_{n}$
24	1	numberical	numerical
27	14	Numberical	Numerical
40	2	form	forms
40	5	that the present	that in the present
41	23	predominately	predominantly
43	6	μ are computed	μ as computed
44	8	form	from
49	1	$\frac{dP_{\tau}^{m}}{d\theta}$	$\frac{dP_{\tau'}^{m}}{d\theta}$
54	6	vary	varies

THE SCATTERING OF A PLANE ELECTROMAGNETIC WAVE BY A FINITE CONE

Introduction

The scattering and/or diffraction of electromagnetic waves by various objects has long been of considerable interest to scientists and engineers from both a practical and a theoretical viewpoint. Since, however, the exact determination of the scattering of electromagnetic waves by bodies other than those having very simple shapes involves considerable difficulty, a number of approximate theories have been developed which may generally be classed according to the range of wavelength to dimension-of-object ratio. Among these are the Rayleigh[1] theory, Fock[2] theory, Franz[3] (creeping wave) theory, and the theories of physical and geometrical optics. An excellent summary and application of these methods appears in a paper by K. M. Siegel[4].

Approximate theories cannot be applied, however, when the dimensions of the scattering object are in the neighborhood of a wavelength. For this so-called "resonance" region, only exact theory (i.e., a solution of Maxwell's equations) applies.

Due to the difficulty of obtaining exact solutions, the problems which have been solved using exact theory are notably few. Of bodies which are infinite in extent, solutions have been obtained for the cylinder by both Seitz[5] and Ignatowsky[6], the semi-infinite plane by Sommerfeld[7], the wedge by Oberhettinger[8], the cone by Hansen and Schiff[9], and the parabaloid by Horton and Karal[10]. Finite bodies for which solutions exist are the sphere (by Mie[11]), the prolate spheroid (by Schultz[12]), and the disk (by Moglich[13], Spence[14], and Meixner[15]). The works of Siegel[16] are also particularly

notable for the reduction of some of the above solutions to useful numerical results.

One of the outstanding features of nearly all of these problems is the fact that the surface of the scattering object may be described by fixing one coordinate of a coordinate system in which the wave equation is separable. Here, indeed, lies one of the prime difficulties in obtaining exact solutions: the fact that one is persistently restricted to the use of a separable scalar wave equation, and consequently to the eleven coordinate systems in which this equation is separable. Furthermore, only a fraction of these systems involve well-known functions for which information is readily available.

It was with the foregoing thoughts in mind that a project was undertaken to attempt to develop a method for the exact determination of the fields scattered from irregularly shaped objects.

As with all electromagnetic boundary-value problems, an exact solution to Maxwell's equations consists of finding a solution subject to (1) the boundary conditions at the surface of the object, (2) the radiation condition at infinity, and (3) the finite energy condition. For general irregular scattering objects, the first two conditions introduce an additional difficulty since the radiation condition is always of a spherical nature (for finite-sized objects), and the surface of the scatterer will not in general be such. The third condition is usually implied when singular functions are discarded from use in the field expansions about smooth objects, and becomes of much greater concern when dealing with bodies with sharp edges and tips.

Preliminary Discussion of the Problem

As a first step in the treatment of irregularly shaped objects, the problem undertaken herein is concerned with the exact solution for the scattering of a plane electromagnetic wave by a finite-sized perfectly conducting cone. Papers by Siegel[4,17] and Keller[18] have previously treated the finite cone using the approximate theories of Rayleigh and physical optics, and geometrical optics, respectively. We consider here only "nose-on" incidence (see fig. 1), and, in order to retain a spherical system throughout, the end-cap of the cone will be assumed to be a spherical sector.

We seek a solution of the vector Helmholtz equation,

$$\nabla^2 \bar{C} + k^2 \bar{C} = 0, \tag{1}$$

where $k = 2\pi/\lambda$ and $\bar{C}$ may be either the electric or the magnetic field vector, $\bar{E}$ or $\bar{H}$. It is commonly known that if Φ is a solution of the scalar wave equation,

$$\nabla^2 \Phi + k^2 \Phi = 0, \tag{2}$$

then the functions, $\bar{l}$, $\bar{m}$, and $\bar{n}$, defined by

$$\begin{aligned} \bar{l} &= \text{grad } \Phi, \\ \bar{m} &= \text{curl } \Phi \bar{a}_r, \\ \bar{n} &= \frac{1}{k} \text{curl } \bar{m}, \end{aligned} \tag{3}$$

are solutions of (1) and form the basis for the most general solution of (1) (Ref. 25, p. 1766). Here, $\bar{a}_r$ is the unit radial vector in spherical coordinates. Since, for the case under consideration, div $\bar{E}$ = div $\bar{H}$ = 0, and since div $\bar{l} \neq 0$, only $\bar{m}$ and $\bar{n}$ need to be used in the expansions

PHYSICAL CONFIGURATION

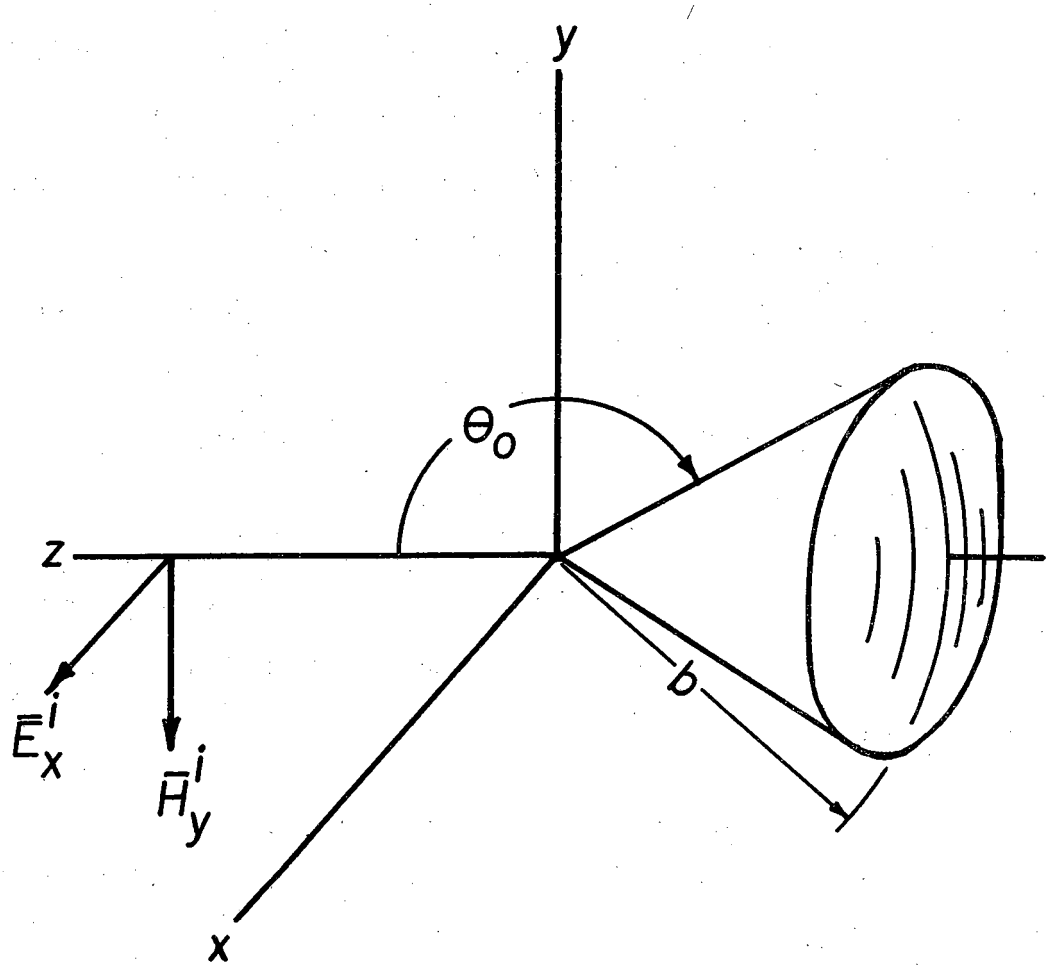

Figure 1

of the field quantities.

In spherical coordinates, equation (2) becomes

$$\frac{1}{r^2}\frac{\partial}{\partial r}\left(r^2\frac{\partial\Phi}{\partial r}\right) + \frac{1}{r^2\sin\theta}\frac{\partial}{\partial\theta}\left(\sin\theta\frac{\partial\Phi}{\partial\theta}\right) + \frac{1}{r^2\sin^2\theta}\frac{\partial^2\Phi}{\partial\Phi^2} + k^2\Phi = 0, \qquad (4)$$

which, when letting $\Phi(r,\theta,\phi) = f_1(r)f_2(\theta)f_3(\phi)$, separates into

$$\frac{1}{r}\frac{d^2(rf_1)}{dr^2} + \left[k^2 - \frac{\upsilon(\upsilon+1)}{r^2}\right]f_1 = 0, \qquad (5)$$

$$\frac{1}{\sin\theta}\frac{d}{d\theta}\left(\sin\theta\frac{df_2}{d\theta}\right) + \left[\upsilon(\upsilon+1) - \frac{m^2}{\sin^2\theta}\right]f_2 = 0, \qquad (6)$$

$$\frac{d^2f_3}{d\phi^2} + m^2f_3 = 0, \qquad (7)$$

where $\upsilon(\upsilon+1)$ and m^2 are separation constants. The solutions of these equations are, respectively,

$$f_1(r) = z_\upsilon(kr) = \sqrt{\pi/(2kr)}\;\; Z_{\upsilon+1/2}(kr), \qquad (8)$$

$$f_2(\theta) = P_\upsilon^m(\cos\theta), \qquad (9)$$

$$f_3(\phi) = \begin{bmatrix}\cos m\phi \\ \sin m\phi,\end{bmatrix} \qquad (10)$$

where $z_\upsilon(kr)$ is a spherical Bessel or Hankel function of order υ, $Z_{\upsilon+1/2}(kr)$ the corresponding cylindrical function, and $P_\upsilon^m(\cos\theta)$ is the associated Legendre function of degree υ and order m. For physical fields in the complete ϕ domain, m must be zero or an integer. Consequently,

$$\Phi^n_{\substack{e\\o}\upsilon m}(r,\theta,\phi) = f_1f_2f_3 = z^n_\upsilon(kr)\,P^m_\upsilon(\cos\theta)\begin{bmatrix}\cos m\phi \\ \sin m\phi\end{bmatrix} \qquad (11)$$

where we let "e" (even) or "o" (odd) indicate cos mϕ or sin mϕ, respectively, and n may take on the values 1, 2, 3, or 4, where these numbers represent Bessel functions of the first and second kind, and

Hankel functions of the first and second kind, respectively; that is

$$z_\upsilon^1(kr) = j_\upsilon(kr), \qquad z_\upsilon^2(kr) = n_\upsilon(kr),$$
$$z_\upsilon^3(kr) = h_\upsilon^1(kr), \qquad z_\upsilon^4(kr) = h_\upsilon^2(kr). \tag{12}$$

From (11) and (3), we obtain

$$\bar{M}_{\substack{e\\o}m\upsilon}^{(n)} = \mp \frac{m}{\sin\theta} z_\upsilon^n(kr) P_\upsilon^m(\cos\theta) \begin{matrix}\sin m\phi\\ \cos m\phi\end{matrix} \bar{a}_\theta - z_\upsilon^n(kr) \frac{\partial P_\upsilon^m}{\partial\theta} \begin{matrix}\cos m\phi\\ \sin m\phi\end{matrix} \bar{a}_\phi \tag{13}$$

$$\bar{N}_{\substack{e\\o}m\upsilon}^{(n)} = \frac{\upsilon(\upsilon+1)}{kr} z_\upsilon^n(kr) P_\upsilon^m(\cos\theta) \begin{matrix}\cos m\phi\\ \sin m\phi\end{matrix} \bar{a}_r + z_\upsilon^{n'}(kr) \frac{\partial P_\upsilon^m}{\partial\theta} \begin{matrix}\cos m\phi\\ \sin m\phi\end{matrix} \bar{a}_\theta \mp \frac{m}{\sin\theta} z_\upsilon^{n'}(kr) P_\upsilon^m(\cos\theta) \begin{matrix}\sin m\phi\\ \cos m\phi\end{matrix} \bar{a}_\phi \tag{14}$$

where $z_\upsilon^{n'}(kr) = \frac{1}{kr}\frac{d}{dr}[rz_\upsilon^n(kr)]$, and $\bar{a}_r$, $\bar{a}_\theta$, and $\bar{a}_\phi$ are unit vectors.

For the particular representation of our field quantities, it will later become evident that it is convenient to split the space surrounding the cone into various regions; however, there exist two logical choices for such a division: one corresponding to the physical regions and the other to a coordinate surface (see fig. 2). The division of the surrounding space corresponding to the physical regions has been used by Sommerfeld[19] in the treatment of the semi-infinite plane and by others in the treatment of semi-infinite bodies. Since we will be using spherical harmonic expansions, however, there are numerous reasons for choosing the division utilizing the coordinate surface.

Since the radiation condition must be satisfied for the scattered

fields, the use of Hankel functions is immediately suggested since they possess the desired behavior as $r \rightarrow \infty$. The Hankel functions possess a logarithmic singularity at $r = 0$, however, which is too large for satisfaction of the finite energy condition at the tip of the cone. Thus near the tip, the use of Bessel functions is essential. As a result, the behavior of the radial functions suggest a division at some finite value of r.

If one further considers the behavior of the associated Legendre functions, the problem suggests using functions of integral degree (i.e. polynomials) for all $r > b$, since in this region the fields exist and are finite throughout the complete θ domain, and any Legendre function of non-integral degree becomes infinite at either $\theta = 0$ or π. For $r \leq b$, $\theta = \pi$ is not in the domain of interest, and consequently non-integral degree Legendre functions may be used. In addition, as may be seen later, the proper selection of the degree may be used for the satisfaction of the boundary conditions at the surface of the cone.

Thus the θ functions also suggest a division of the exterior region at a finite value of r, namely $r = b$. We thus choose this coordinate division of the exterior space for the solution of our problem. The selection of the functions in the interior region, $r \leq b$, is very similar to that used by Hansen and Schiff[9] in their treatment of the semi-infinite cone. Also, the division of the exterior space by the coordinate surface $r = b$ is analogous to the choice of Schelkunoff[20] in treating the biconical antenna.

One may then raise the question as to whether or not a division of the exterior region into three sub-regions as shown in figure 3 would be more advantageous. In such a case, the associated Legendre functions of

SPACE SECTIONALIZING

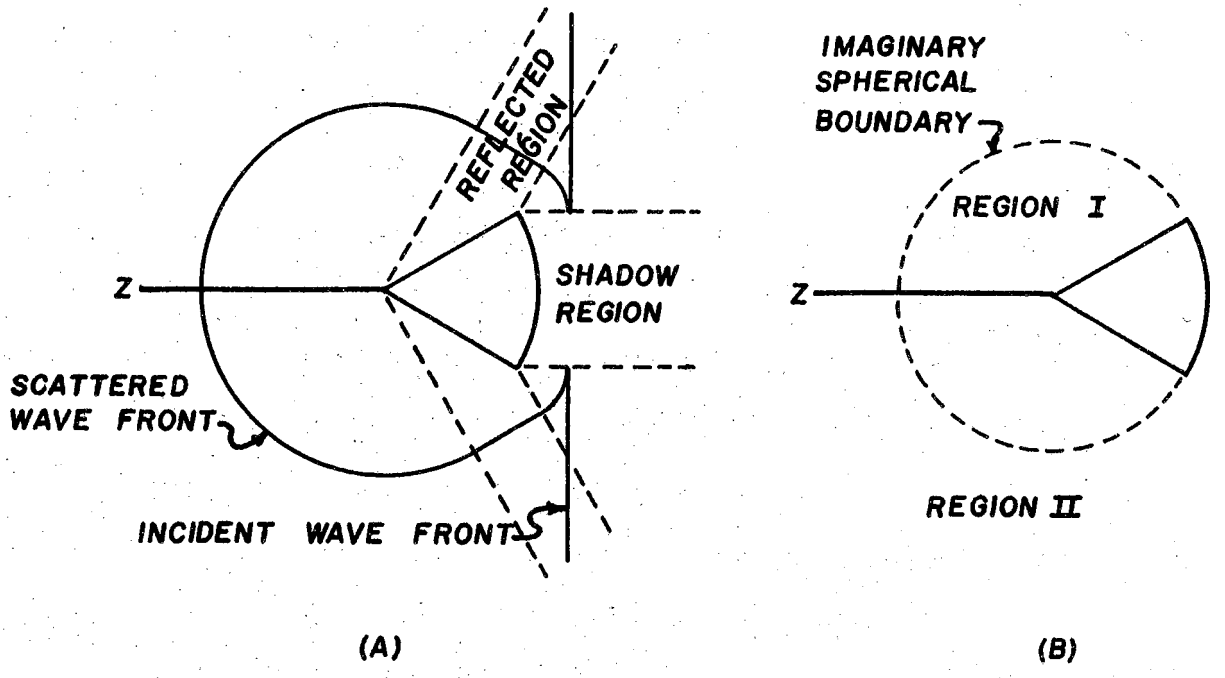

Figure 2

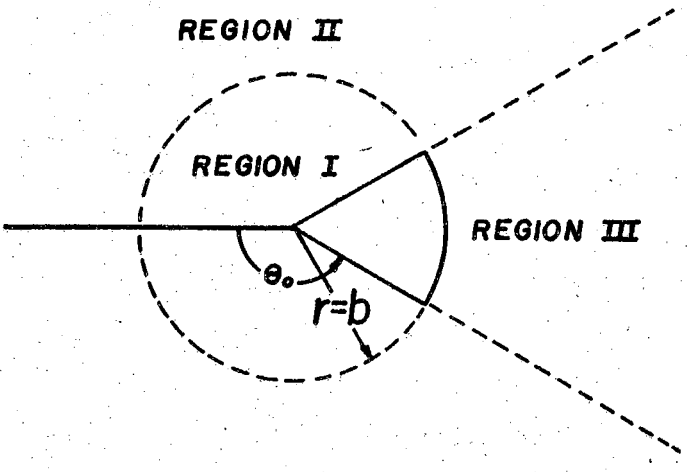

Figure 3

non-integral degree and a positive argument (i.e. $P_\mu^m(\cos\theta)$) could be used in region II, and similar functions with a negative argument, $P_\upsilon^m(-\cos\theta)$, could be used in region III, thus maintaining finite functions throughout all space. The primary advantage in such a choice ultimately leads to the use of functions orthogonal in both r and θ, and the resulting finality of the expansion coefficients: certainly, this would be a most desirable feature. Although such a choice may be possible (see Appendix A), the resulting equation for the determination of υ in (11) becomes so involved that it is believed to be less adaptable to numerical computation than the non-finality of the coefficients that is ultimately obtained in the present solution.

We proceed, therefore, with a regional sectionalizing as indicated in figure 2b.

Field Expansions

We begin by considering the expansions for the electric fields. A time variation of $e^{+i\omega t}$ is assumed throughout.

In region II, the incident electric field may be expressed (ref. 3, p. 419)

$$\bar{E}_{II}^{i} = \bar{a}_x e^{ikz} = \bar{a}_x e^{ikr\cos\theta} = \sum_n \left(\gamma_n \bar{m}_{oln}^{(1)} + \mathscr{J}_n \bar{n}_{eln}^{(1)}\right), \qquad (15)$$

where

$$\gamma_n = i^n \frac{2n+1}{n(n+1)}, \quad \mathscr{J}_n = -i^{n+1} \frac{2n+1}{n(n+1)},$$

and $\bar{a}_x$ is a unit vector in the x direction.

In this case, the summation is over all of the integers, n, from one to infinity. Consideration of the ϕ variation of the incident field led to the choice of the even $\bar{m}$ and odd $\bar{n}$ functions for the expansion,

and the Φ variation also limits us to $m = 1$. As a result, we will use even $\bar{m}$ and odd $\bar{n}$ functions with $m = 1$ for all expansions of the electric fields.

In region I we are not necessarily interested in the separate incident and scattered fields, and will thus assume an expansion of the total field only. Consideration of the previous arguments about the radial functions and Legendre functions leads us to choose an expansion of the form

$$\bar{E}_I^t = \sum_{\upsilon} a_\upsilon \bar{m}_{o1\upsilon}^{(1)} + \sum_{\mu} b_\mu \bar{n}_{e1\mu}^{(1)}, \tag{16}$$

where a_υ and b_μ are expansion coefficients to be determined by the boundary conditions of the problem, and μ and υ are the non-integral degrees of the associated Legendre functions which are also yet to be determined.

For the scattered field in the exterior region, the prior arguments lead to the choice

$$\bar{E}_{II}^s = \sum_{n} (c_n \bar{m}_{o1n}^{(4)} + d_n \bar{n}_{e1n}^{(4)}), \tag{17}$$

where c_n and d_n are constants to be determined. Here we have selected $z_n^4(kr) = h_n^2(kr)$, the Hankel function of the second kind, since it possesses an asymptotic form

$$h_n^2(kr) \to \frac{1}{kr} i^{(n+1)} e^{-ikr} \tag{18}$$

$$kr \to \infty$$

and will thus represent an outward traveling wave at infinity and satisfy the radiation condition. Hereafter, since we will use only the Hankel function of the second kind, the superscript will be omitted and assumed to be understood.

The Problem Solution

The equations (16) and (17) thus contain six unknown sets of constants which must be determined; namely, $\mu, \upsilon, a_\upsilon, b_\mu, c_n$, and d_n.

Through the judicious choice of functions, we have already insured the satisfaction of the finite energy condition at the tip of the cone and the radiation condition at infinity. There remain, then, the following boundary conditions:

(1) $[\overline{E}^{t}_{I}]_{r,\phi} = 0$ at $\theta = \theta_o$, $r \leq b$; (19a)

(2) $[\overline{E}^{i}_{II} + \overline{E}^{s}_{II}]_{\theta,\phi} = 0$ at $r = b$, $\theta_o \leq \theta \leq \pi$; (19b)

(3) $[\overline{E}^{i}_{II} + \overline{E}^{s}_{II}]_{\theta,\phi} = [\overline{E}^{t}_{I}]_{\theta,\phi}$ (19c)

$[\overline{H}^{i}_{II} + \overline{H}^{s}_{II}]_{\theta,\phi} = [\overline{H}^{t}_{I}]_{\theta,\phi}$ (19d)

} at $r = b$, $0 \leq \theta < \theta_o$;

(4) The finite energy condition at the edge of the cone,

$r \to b$, $\theta \to \theta_o$, (19f)

where b is the radius of the spherical end cap and θ_o is half of the exterior apex angle.

The third condition insures the continuity of the field components across the imaginary spherical boundary.

For further reference, we state the Maxwell equations,

$$\text{curl } \overline{E} = -i\omega\mu_o \overline{H}, \qquad \text{curl } \overline{H} = i\omega\epsilon_o \overline{E}; \tag{20}$$

and the relations,

$$\text{curl } \overline{m} = k\overline{n}, \qquad \text{curl } \overline{n} = k\overline{m}. \tag{21}$$

From equations (15) thru (17), (20) and (21), and noting also that $k = \omega\sqrt{\mu_o \epsilon_o}$, one easily obtains the expressions for the magnetic fields:

$$\bar{H}^{i}_{II} = \frac{i}{\eta}\left[\sum_n (\gamma_n \bar{n}^{(1)}_{oln} + \mathcal{J}_n \bar{m}^{(1)}_{eln})\right], \tag{22}$$

$$\bar{H}^{t}_{I} = \frac{i}{\eta}\left[\sum_\upsilon a_\upsilon \bar{n}^{(1)}_{olv} + \sum_\mu b_\mu \bar{m}^{(1)}_{el\mu}\right], \tag{23}$$

$$\bar{H}^{s}_{II} = \frac{i}{\eta}\left[\sum_n (c_n \bar{m}^{(4)}_{oln} + d_n \bar{m}^{(4)}_{eln})\right], \tag{24}$$

where η is the intrinsic impedance of free space, $\sqrt{\mu_o/\epsilon_o}$.

Again for future reference, the field quantities are expanded in their entirety below.

$$\begin{aligned}\bar{E}^{t}_{I} = &\left[\sum_\mu b_\mu \frac{\mu(\mu+1)}{kr} j_\mu(kr) P^1_\mu(\cos\theta)\right]\cos\phi\ \bar{a}_r \\ &+ \left[\sum_\upsilon a_\upsilon j_\upsilon(kr)\frac{P^1_\upsilon(\cos\theta)}{\sin\theta} + \sum_\mu b_\mu j'_\mu(kr)\frac{dP^1_\mu}{d\theta}\right]\cos\phi\ \bar{a}_\theta \\ &- \left[\sum_\upsilon a_\upsilon j_\upsilon(kr)\frac{dP^1_\upsilon}{d\theta} + \sum_\mu b_\mu j'_\mu(kr)\frac{P^1_\mu(\cos\theta)}{\sin\theta}\right]\sin\phi\ \bar{a}_\phi .\end{aligned} \tag{25}$$

$$\begin{aligned}\bar{E}^{i}_{II} = \sum_n \Bigg\{ &\left[\mathcal{J}_n \frac{n(n+1)}{kr} j_n(kr) P^1_n(\cos\theta)\right]\cos\phi\ \bar{a}_r \\ &+ \left[\gamma_n j_n(kr)\frac{P^1_n(\cos\theta)}{\sin\theta} + \mathcal{J}_n j'_n(kr)\frac{dP^1_n}{d\theta}\right]\cos\phi\ \bar{a}_\theta \\ &- \left[\gamma_n j_n(kr)\frac{dP^1_n}{d\theta} + \mathcal{J}_n j'_n(kr)\frac{P^1_n(\cos\theta)}{\sin\theta}\right]\sin\phi\ \bar{a}_\phi \Bigg\} .\end{aligned} \tag{26}$$

$$\begin{aligned}\bar{E}^{s}_{II} = \sum_n \Bigg\{ &\left[d_n \frac{n(n+1)}{kr} h_n(kr) P^1_n(\cos\theta)\right]\cos\phi\ \bar{a}_r \\ &+ \left[c_n h_n(kr)\frac{P^1_n(\cos\theta)}{\sin\theta} + d_n h'_n(kr)\frac{dP^1_n}{d\theta}\right]\cos\phi\ \bar{a}_\theta \\ &- \left[c_n h_n(kr)\frac{dP^1_n}{d\theta} + d_n h'_n(kr)\frac{P^1_n(\cos\theta)}{\sin\theta}\right]\sin\phi\ \bar{a}_\phi \Bigg\} .\end{aligned} \tag{27}$$

$$\bar{H}_I^t = \frac{i}{\eta} \left[\sum_\upsilon a_\upsilon \frac{\upsilon(\upsilon+1)}{kr} j_\upsilon(kr) P_\upsilon^1(\cos\theta) \sin\phi \, \bar{a}_r \right.$$

$$+ \sum_\upsilon a_\upsilon j_\upsilon'(kr) \frac{dP_\upsilon^1}{d\theta} - \sum_\mu b_\mu j_\mu(kr) \frac{P_\mu^1(\cos\theta)}{\sin\theta} \sin\phi \, \bar{a}_\theta \qquad (28)$$

$$\left. + \sum_\upsilon a_\upsilon j_\upsilon'(kr) \frac{P_\upsilon^1(\cos\theta)}{\sin\theta} - \sum_\mu b_\mu j_\mu(kr) \frac{dP_\mu^1}{d\theta} \cos\phi \, \bar{a}_\phi \right].$$

$$\bar{H}_{II}^i = \frac{i}{\eta} \sum_n \left\{ \left[\gamma_n \frac{n(n+1)}{kr} j_n(kr) P_n^1(\cos\theta) \right] \sin\phi \, \bar{a}_r \right.$$

$$+ \left[\gamma_n j_n'(kr) \frac{dP_n^1}{d\theta} - \mathcal{T}_n j_n(kr) \frac{P_n^1(\cos\theta)}{\sin\theta} \right] \sin\phi \, \bar{a}_\theta \qquad (29)$$

$$\left. + \left[\gamma_n j_n'(kr) \frac{P_n^1(\cos\theta)}{\sin\theta} - \mathcal{T}_n j_n(kr) \frac{dP_n^1}{d\theta} \right] \cos\phi \, \bar{a}_\phi \right\}.$$

$$\bar{H}_{II}^s = \frac{i}{\eta} \sum_n \left\{ \left[c_n \frac{n(n+1)}{kr} h_n(kr) P_n^1(\cos\theta) \right] \sin\phi \, \bar{a}_r \right.$$

$$+ \left[c_n h_n'(kr) \frac{dP_n^1}{d\theta} - d_n h_n(kr) \frac{P_n^1(\cos\theta)}{\sin\theta} \right] \sin\phi \, \bar{a}_\theta \qquad (30)$$

$$\left. + \left[c_n h_n'(kr) \frac{P_n^1(\cos\theta)}{\sin\theta} - d_n h_n(kr) \frac{dP_n^1}{d\theta} \right] \cos\phi \, \bar{a}_\phi \right\}.$$

We now begin by applying the boundary conditions at the surface of the cone.

To satisfy (19a), we equate the r-component of $\bar{E}_I^t$ to zero at $\theta = \theta_o$,

$$\sum_\mu b_\mu \frac{\mu(\mu+1)}{kr} j_\mu(kr) P_\mu^1(\cos\theta_o) = 0, \qquad (31)$$

and thus set

$$P_\mu^1(\cos\theta_o) = 0. \qquad (32)$$

This equation thus determines the values of μ. Equating the ϕ-component of $\overline{E}_I^t$ to zero gives

$$\sum_{\upsilon} a_{\upsilon} j_{\upsilon}(kr) \left.\frac{dP_{\upsilon}^1}{d\theta}\right|_{\theta=\theta_o} + \sum_{\mu} b_{\mu} j'_{\mu}(kr) \frac{P_{\mu}^1(\cos\ \theta_o)}{\sin\ \theta_o} = 0. \tag{33}$$

Since $P_{\mu}^1(\cos\ \theta_o) = 0$, we set

$$\left.\frac{dP_{\upsilon}^1}{d\theta}\right|_{\theta=\theta_o} = 0. \tag{34}$$

and thus determine values of υ.

From (19b), (26), and (27), we have for $r = b$, $\theta_o \leq \theta \leq \pi$,

$$\sum_{n} \left\{ [\gamma_n j_n(kb) + c_n h_n(kb)] \frac{P_n^1(\cos\theta)}{\sin\theta} + [\gamma_n j'_n(kb) + d_n h'_n(kb)] \frac{dP_n^1}{d\theta} \right\} = 0, \tag{35}$$

for the θ-component, and, for the ϕ component,

$$\sum_{n} \left\{ [\gamma_n j_n(kb) + c_n h_n(kb)] \frac{dP_n^1}{d\theta} + [\gamma_n j'_n(kb) + d_n h'_n(kb)] \frac{P_n^1(\cos\theta)}{\sin\theta} \right\} = 0. \tag{36}$$

These two equations contain the unknowns c_n and d_n and apply over a portion of the θ domain. In order to obtain equations involving only one set of coefficients, we first multiply (35) by $\sin\theta$ and then differentiate with respect to θ; there results

$$\sum_{n} \left\{ [\gamma_n j_n(kb) + c_n h_n(kb)] \frac{dP_n^1}{d\theta} + [\gamma_n j'_n(kb) + d_n h'_n(kb)] \frac{d}{d\theta}\left(\sin\theta\ \frac{dP_n^1}{d\theta}\right) \right\} = 0. \tag{37}$$

The subtraction of (37) from (37) yields

$$\sum_n [\mathscr{T}_n j'_n(kb) + d_n h'_n(kb)] \left\{ - \frac{d}{d\theta} (\sin \theta \frac{dP^1_n}{d\theta}) + \frac{P^1_n(\cos \theta)}{\sin \theta} \right\} = 0. \tag{38}$$

Furthermore, since the Legendre equation may be expressed as

$$\frac{d}{d\theta} (\sin \theta \frac{dP^m_\upsilon}{d\theta}) - \frac{m^2}{\sin \theta} P^m_\upsilon(\cos \theta) = - \upsilon(\upsilon + 1) \sin \theta P^m(\cos \theta); \tag{39}$$

and noting that in this particular case, $\upsilon = n$, $m = 1$, (38) may be written

$$\sum_n n(n + 1) [\mathscr{T}_n j'_n(kb) + d_n h'_n(kb)] \sin \theta P^1_n(\cos \theta) = 0. \tag{40}$$

Since $\sin \theta$ does not depend on the summation index n, it may be removed from the summation and canceled from the equation. Let us signify the first N terms of the resulting series as $S_N(\theta)$, i.e.,

$$S_N(\theta) = \sum_{n=1}^{N} n(n + 1) [\mathscr{T}_n j_n(kb) + d_n h_n(kb)] P^1_n(\cos \theta), \tag{41}$$

$$S_\infty(\theta) = 0; \qquad \theta_o \leq \theta \leq \pi.$$

In a similar manner, we may multiply (36) by $\sin \theta$, then differentiate with respect to θ, and subtract the resulting equation from (35). There results

$$T_N(\theta) = \sum_{n=1}^{N} n(n + 1) [\gamma_n j_n(kb) + c_n h_n(kb)] P^1_n(\cos \theta), \tag{42}$$

$$T_\infty(\theta) = 0; \qquad \theta_o \leq \theta \leq \pi.$$

We have thus obtained two equations involving the unknown coefficients c_n and d_n for a portion of the range of θ.

Next, we will apply (19c). From (25) through (27), we have for the θ-component, where $r = b$, $0 \leq \theta < \theta_o$:

$$\sum_\upsilon a_\upsilon j_\upsilon(kb) \frac{P_\upsilon^1(\cos\theta)}{\sin\theta} + \sum_\mu b_\mu j'_\mu(kb) \frac{dP_\mu^1}{d\theta}$$

$$= \sum_n \left\{ [\gamma_n j_n(kb) + c_n h_n(kb)] \frac{P_n^1(\cos\theta)}{\sin\theta} + [\delta_n j'_n(kb) + d_n h'_n(kb)] \frac{dP_n^1}{d\theta} \right\}, \tag{43}$$

and for the ϕ-component,

$$\sum_\upsilon a_\upsilon j_\upsilon(kb) \frac{dP_\upsilon^1}{d\theta} + \sum_\mu b_\mu j'_\mu(kb) \frac{P_\mu^1(\cos\theta)}{\sin\theta} \tag{44}$$

$$= \sum_n \left\{ [\gamma_n j_n(kb) + c_n h_n(kb)] \frac{dP_n^1}{d\theta} + [\delta_n j'_n(kb) + d_n h'_n(kb)] \frac{P_n^1(\cos\theta)}{\sin\theta} \right\}.$$

In a manner exactly analogous to that used in obtaining equation (40), we may first multiply (44) by $\sin\theta$, differentiate with respect to θ, and subtract the resulting equation from (43). There then results

$$\sum_\upsilon a_\upsilon j_\upsilon(kb)\, \upsilon(\upsilon+1)\, \cancel{\sin\theta}\, P_\upsilon^1(\cos\theta)$$

$$= \sum_n [\gamma_n j_n(kb) + c_n h_n(kb)]\, n(n+1)\, \cancel{\sin\theta}\, P_n^1(\cos\theta) \tag{45}$$

$$= T_\infty(\theta); \qquad 0 \leq \theta < \theta_o.$$

Performing the same operations on (43) and subtracting the results from (44) yields

$$\sum_\mu b_\mu j'_\mu(kb)\, \mu(\mu+1)\, \cancel{\sin\theta}\, P_\mu^1(\cos\theta)$$

$$= \sum_n [\delta_n j'_n(kb) + d_n h'_n(kb)]\, n(n+1)\, \cancel{\sin\theta}\, P_n^1(\cos\theta) \tag{46}$$

$$= S_\infty(\theta); \qquad 0 \leq \theta < \theta_o.$$

Considering (40) and (46), let us define a function $f(\theta)$ as follows:

$$f(\theta) = \begin{cases} \sum_\mu b_\mu j'_\mu(kb)\, \mu(\mu+1)\, P_\mu^1(\cos\theta), & 0 \leq \theta < \theta_o, \\ 0, & \theta_o \leq \theta \leq \pi. \end{cases} \tag{47}$$

We may now think of $f(\theta)$ as a defined function which we would like to represent as accurately as possible by a finite series, $S_N(\theta)$, and then minimize a weighted mean square error to find the coefficients d_n in terms of the b_μ coefficients (Ref. 21, p. 1ff).

Let $\epsilon(\theta) = f(\theta) - S_N(\theta)$ represent the error, and then form the mean square error weighted by an amount $\sin\theta$, thus:

$$M = \frac{1}{\pi}\int_0^\pi \epsilon^2(\theta)\,\sin\theta\,d\theta. \tag{48}$$

Since this weighting factor is always positive in the range of integration, $0 - \pi$, it does not destroy the primary significance of M, but only causes the error in the center of the range to be weighted more heavily than that at the end points (Ref. 21, p. 26).

In order to minimize the mean square error with respect to a particular coefficient d_m, we form

$$-\frac{\partial M}{\partial d_m} = \frac{1}{\pi}\int_0^\pi 2[f(\theta)-S_N(\theta)]\,h_m'(kb)m(m+1)P_m^1(\cos\theta)\sin\theta\,d\theta = 0. \tag{49}$$

If we now insert the expression for $S_N(\theta)$ into the equation and move the portion containing that series to the right-hand side, the orthogonality of the associated Legendre functions produces

$$\int_0^\pi f(\theta)P_m^1(\cos\theta)\sin\theta\,d\theta \tag{50}$$

$$= [\mathcal{J}_m j_m'(kb) + d_m h_m'(kb)]\,m(m+1)\int_0^\pi \sin\theta\,[P_m^1(\cos\theta)]^2\,d\theta,$$

after canceling $\frac{2}{\pi}\,m(m+1)h_m'(kb)$. Inserting the expression for $f(\theta)$ and evaluating the integral on the right side, one obtains

$$\sum_{\mu} b_{\mu} j'_{\mu}(kb)\mu(\mu+1) \int_{0}^{\theta_o} \sin\theta\, P_{\mu}^{1}(\cos\theta)\, P_{m}^{1}(\cos\theta)\, d\theta$$

$$= [\mathcal{J}_m j'_m(kb) + d_m h_m(kb)\,] \frac{2[m(m+1)]^2}{2m+1}\,. \tag{51}$$

One may evaluate the integral on the left (Ref. 22, p. 431):

$$\int_{0}^{\theta_o} P_{\mu}^{1}(\cos\theta)\, P_{m}^{1}(\cos\theta)\, \sin\theta\, d\theta$$

$$= \frac{\sin\theta_o}{m(m+1) - \mu(\mu+1)} \left[P_{m}^{1}(\cos\theta) \frac{dP_{\mu}^{1}}{d\theta} - P_{\mu}^{1}(\cos\theta) \frac{dP_{m}^{1}}{d\theta} \right] \Bigg|_{0}^{\theta_o} \tag{52}$$

$$= \frac{\sin\theta_o}{m(m+1) - \mu(\mu+1)}\, P_{m}^{1}(\cos\theta_o) \left.\frac{dP_{\mu}^{1}}{d\theta}\right|_{\theta=\theta_o}.$$

After replacing the integral in (51) by (52) and then solving for the coefficient d_m, one obtains

$$d_m = \frac{2m+1}{m(m+1)} \frac{j'_m(kb)}{h'_m(kb)} \left[\frac{1}{2} \sin\theta_o\, P_{m}^{1}(\cos\theta_o) \right. \tag{53}$$

$$\left. x \sum_{\mu} b_{\mu} \frac{j'_{\mu}(kb)}{j'_m(kb)} \frac{\mu(\mu+1)}{m(m+1)} \frac{1}{m(m+1) - \mu(\mu+1)} \left.\frac{dP_{\mu}^{1}}{d\theta}\right|_{\theta=\theta_o} + i^{m+1} \right].$$

In a similar manner, we may define a function $g(\theta)$ over the range $0 - \pi$ by considering equations (42) and (45):

$$g(\theta) = \begin{cases} \sum_{\upsilon} a_{\upsilon} j_{\upsilon}(kb)\upsilon(\upsilon+1) P_{\upsilon}^{1}(\cos\theta), & 0 \le \theta < \theta_o, \\ 0, & \theta_o \le \theta \le \pi\,. \end{cases} \tag{54}$$

We thus wish to represent $g(\theta)$ by the series $T_N(\theta)$, and will, in an analogous manner to that used before, form an error, $\delta(\theta) = g(\theta) - T_N(\theta)$, and then minimize the mean square error,

$$M = \frac{1}{\pi} \int_{0}^{\pi} \delta^{2}(\theta) \sin\theta\, d\theta, \tag{55}$$

with respect to a particular coefficient, c_m: there results

$$-\frac{\partial M}{\partial c_m} = \frac{1}{\pi}\int_o^{\pi} 2[g(\theta) - T_N(\theta)]h_m(kb)m(m+1)P_m^1(\cos\theta)\sin\theta\ d\theta = 0. \tag{56}$$

Evaluating the integrals yields

$$\sin\theta_o \left.\frac{dP_m^1}{d\theta}\right|_{\theta=\theta_o} \sum_{\upsilon} a_\upsilon j_\upsilon(kb)\upsilon(\upsilon+1)\frac{P_\upsilon^1(\cos\theta_o)}{\upsilon(\upsilon+1)-m(m+1)} = [\gamma_m j_m(kb)+c_m h_m(kb)]\frac{2[m(m+1)]^2}{2m+1} \tag{57}$$

and upon solving for c_m, one obtains

$$c_m = \frac{2m+1}{m(m+1)}\frac{j_m(kb)}{h_m(kb)}\left[\frac{1}{2}\sin\theta_o \left.\frac{dP_m^1}{d\theta}\right|_{\theta\,\theta_o} \sum_{\upsilon} a_\upsilon \frac{j_\upsilon(kb)}{j_m(kb)}\ \upsilon(\upsilon+1)\ \frac{P_\upsilon^1(\cos\theta_o)}{\upsilon(\upsilon+1)-m(m+1)} - i^m\right]. \tag{58}$$

Let us now apply the same technique to the tangential magnetic fields over the imaginary spherical boundary. By minimizing the errors with respect to a_υ and b_μ, one may obtain expressions for these coefficients in terms of the coefficients c_n and d_n, which upon substitution into equations (53) and (58), will yield an infinite set of equations for the coefficients c_n and d_n. The reverse substitution will also produce a similar set of equations for the coefficients a_υ and b_μ. To this end, we have from (19d) and (22) thru (24) for the θ-component in the region $0 \le \theta < \theta_o$,

$$\sum_{\upsilon} a_\upsilon j_\upsilon'(kb)\frac{dP_\upsilon^1}{d\theta} - \sum_{\mu} b_\mu j_\mu(kb)\frac{P_\mu^1(\cos\theta)}{\sin\theta} = \sum_n\left\{[\gamma_n j_n'(kb) + c_n h_n'(kb)]\frac{dP_n^1}{d\theta} - [\gamma_n j_n(kb) + d_n h_n(kb)]\frac{P_n^1(\cos\theta)}{\sin\theta}\right\}, \tag{59}$$

and for the ϕ-component

$$\sum_{\upsilon} a_\upsilon j_\upsilon'(kb)\frac{P_\upsilon^1(\cos\theta)}{\sin\theta} - \sum_{\mu} b_\mu j_\mu(kb)\frac{dP_\mu^1}{d\theta} = \sum_n\left\{[\gamma_n j_n'(kb) + c_n h_n'(kb)]\frac{P_n^1(\cos\theta)}{\sin\theta} - [\gamma_n j_n(kb) + d_n h_n(kb)]\frac{dP_n^1}{d\theta}\right\}. \tag{60}$$

Multiplying (59) by sin θ, differentiating with respect to θ, subtracting the resulting equation from (60) and utilizing the Legendre equation (39) produces

$$\sum_{\upsilon} a_{\upsilon} j'_{\upsilon}(kb)\upsilon(\upsilon+1)P^1_{\upsilon}(\cos\theta) = \sum_{n} [\gamma_n j'_n(kb) + c_n h'_n(kb)]\, n(n+1)P^1_n(\cos\theta). \tag{61}$$

In a like manner, after performing the same operations on equation (60) and subtracting the result from (59), one obtains

$$\sum_{\mu} b_{\mu} j_{\mu}(kb)\mu(\mu+1)P^1_{\mu}(\cos\theta) = \sum_{n}[\gamma_n j_n(kb) + d_n h_n(kb)]\, n(n+1)P^1_n(\cos\theta). \tag{62}$$

We now set

$$\underline{f}(\theta) = \sum_{n} [\gamma_n j_n(kb) + d_n h_n(kb)]\, n(n+1)P^1_n(\cos\theta), \tag{63a}$$

$$S_U(\theta) = \sum_{\mu}^{\mu=U} b_{\mu} j_{\mu}(kb)\mu(\mu+1)P^1_{\mu}(\cos\theta), \tag{63b}$$

$$\underline{\epsilon}(\theta) = \underline{f}(\theta) - S_U(\theta); \tag{63c}$$

$$\underline{g}(\theta) = \sum_{n} [\gamma_n j'_n(kb) + c_n h'_n(kb)]\, n(n+1)P^1_n(\cos\theta), \tag{64a}$$

$$T_V(\theta) = \sum_{\upsilon}^{\upsilon=V} a_{\upsilon} j'_{\upsilon}(kb)\upsilon(\upsilon+1)P^1_{\upsilon}(\cos\theta), \tag{64b}$$

$$\underline{\delta}(\theta) = \underline{g}(\theta) - T_V(\theta). \tag{64c}$$

Forming the mean square errors over the range $0 - \theta_o$,

$$\underline{M} = \frac{1}{\theta_o}\int_0^{\theta_o} \underline{\epsilon}^2(\theta)\sin\theta\, d\theta, \quad \underline{M}' = \frac{1}{\theta_o}\int_0^{\theta_o} \delta^2(\theta)\sin\theta\, d\theta, \tag{65}$$

and minimizing these with respect to b_β and a_α, respectively, where β is a particular μ and α is a particular υ, leads to the equations

$$\sum_n [\mathcal{J}_n j_n(kb) + d_n h_n(kb)]\, n(n+1) \sin\theta_o \left.\frac{dP_\beta^1}{d\theta}\right|_{\theta=\theta_o} \frac{P_n^1(\cos\theta_o)}{n(n+1)-\beta(\beta+1)} \tag{66}$$

$$= b_\beta j_\beta(kb)\beta(\beta+1) \int_o^{\theta_o} \sin\theta [P_\beta^1(\cos\theta)]^2 d\theta,$$

and

$$\sum_n [\gamma_n j_n'(kb) + c_n h_n'(kb)]\, n(n+1) \sin\theta_o \left.\frac{dP_n^1}{d\theta}\right|_{\theta=\theta_o} \frac{P_\alpha^1(\cos\theta_o)}{\alpha(\alpha+1)-n(n+1)} \tag{67}$$

$$= a_\alpha j_\alpha'(kb)\alpha(\alpha+1) \int_o^{\theta_o} \sin\theta\, [P_\alpha^1(\cos\theta)]^2\, d\theta\ .$$

Solving, we obtain

$$b_\beta = \frac{1}{j_\beta(kb)B_\beta} \sum_n [\mathcal{J}_n j_n(kb) + d_n h_n(kb)] \frac{n(n+1)}{\beta(\beta+1)} \left.\frac{dP_\beta^1}{d\theta}\right|_{\theta=\theta_o} \frac{\sin\theta_o P_n^1(\cos\theta_o)}{n(n+1) - \beta(\beta+1)}\ , \tag{68}$$

$$a_\alpha = \frac{1}{j_\alpha(kb)B_\alpha} \sum_n [\gamma_n j_n'(kb) + c_n h_n'(kb)] \frac{n(n+1)}{\alpha(\alpha+1)} \left.\frac{dP_n^1}{d\theta}\right|_{\theta=\theta_o} \frac{\sin\theta_o P_\alpha^1(\cos\theta_o)}{\alpha(\alpha+1) - n(n+1)}\ . \tag{69}$$

where

$$B_\alpha = \int_o^{\theta_o} [P_\alpha^1(\cos\theta_o)]^2 \sin\theta\ d\theta.$$

After the appropriate substitutions, we finally obtain

$$\sum_n \sum_\mu a_\upsilon (a^{\xi n}_{\upsilon\alpha} - a^{K}_{\upsilon}\delta_{\upsilon\alpha}) = \sum_n a^{\psi n}_{\alpha}\ , \tag{70}$$

where

$$a^{\xi n}_{\upsilon\alpha} = \frac{(n+\frac{1}{2})}{n(n+1)} \frac{\upsilon(\upsilon+1)}{\alpha(\alpha+1)} \frac{j_\upsilon(kb)}{h_n(kb)} h_n'(kb) \frac{\sin^2\theta_o P_\upsilon^1(\cos\theta_o) P_\alpha^1(\cos\theta_o)}{[\upsilon(\upsilon+1)-n(n+1)][\alpha(\alpha+1)-n(n+1)]} \left[\left.\frac{dP_n^1}{d\theta}\right|_{\theta=\theta_o}\right]^2,$$

$$a^{\psi n}_{\alpha} = i^n \frac{2n+1}{\alpha(\alpha+1)} \frac{\sin\theta_o P_\alpha^1(\cos\theta_o)}{\alpha(\alpha+1)-n(n+1)} \left.\frac{dP_n^1}{d\theta}\right|_{\theta=\theta_o} \left[\frac{j_n(kb)}{h_n(kb)} h_n'(kb) - j_n'(kb)\right],$$

$$a^{K}_{\upsilon} = j_\upsilon'(kb)B_\upsilon,$$

$$\delta_{\upsilon\alpha} = \begin{cases} 0, \upsilon \neq \alpha \\ 1, \upsilon = \alpha \end{cases}$$

$$\sum_n \sum_\mu {}_b\mu\left({}_b\xi^n_{\mu\beta} - {}_bK_\mu \delta_{\mu\beta}\right) = \sum_n {}_b\psi^n_{\mu\beta}, \tag{71}$$

where

$${}_b\xi^n_{\mu\beta} = \frac{(n+\frac{1}{2})}{n(n+1)} \frac{\mu(\mu+1)}{\beta(\beta+1)} \frac{j'_\mu(kb)}{h'_n(kb)} h_n(kb) \frac{\sin^2\theta_o \left[P^1_n(\cos\theta_o)\right]^2}{\left[n(n+1) - \mu(\mu+1)\right]\left[n(n+1) - \beta(\beta+1)\right]} \left[\frac{dP^1_\mu}{d\theta} \frac{dP^1_\beta}{d\theta}\bigg|_{\theta=\theta_o}\right],$$

$${}_b\psi^n_\beta = i^{n+1} \frac{2n+1}{\beta(\beta+1)} \frac{\sin\theta_o P^1_n(\cos\theta_o)}{\left[n(n+1)-\beta(\beta+1)\right]} \frac{dP^1_\beta}{d\theta}\bigg|_{\theta=\theta_o} \left[\frac{j_n(kb)}{h_n(kb)} h'_n(kb) - j'_n(kb)\right],$$

$${}_bK_\mu = j_\mu(kb)\, B_\mu;$$

$$\sum_\upsilon \sum_n {}_c n\left({}_c\xi^{nm}_\upsilon - {}_cK_n \delta_{mn}\right) = -\sum_\upsilon \sum_n \left({}_a\psi^{nm}_\upsilon - \chi_n \delta_{mn}\right), \tag{72}$$

where

$${}_c\xi^{nm}_\upsilon = \frac{1}{2j_\upsilon(kb)B_\upsilon} \frac{n(n+1)}{m(m+1)} \frac{j_\upsilon(kb)}{h_m(kb)} h'_n(kb) \frac{\sin^2\theta_o \left[P^1_\upsilon(\cos\theta_o)\right]^2}{\left[\upsilon(\upsilon+1)-n(n+1)\right]\left[\upsilon(\upsilon+1)-m(m+1)\right]} \left[\frac{dP^1_m}{d\theta} \frac{dP^1_n}{d\theta}\bigg|_{\theta=\theta_o}\right]$$

$${}_c\psi^{nm}_\upsilon = i^n \frac{2n+1}{n(n+1)} \frac{j'_n(kb)}{h'_n(kb)} {}_c\xi^{nm}_\upsilon,$$

$${}_c\chi_n = i^n \frac{j_n(kb)}{h_n(kb)},$$

$${}_cK_n = \frac{n(n+1)}{2n+1};$$

$$\sum_\mu \sum_n {}_d n\left({}_d\xi^{nm}_\mu - {}_dK_n \delta_{mn}\right) = \sum_\mu \sum_n \left({}_d\psi^{nm}_\mu - {}_d\chi_n \delta_{mn}\right), \tag{73}$$

where

$${}_d\xi^{nm}_\mu = \frac{1}{2j'_\mu(kb)B_\mu} \frac{n(n+1)}{m(m+1)} \frac{j'_\mu(kb)}{h'_m(kb)} h_n(kb) \frac{\sin^2\theta_o P^1_n(\cos\theta_o) P^1_m(\cos\theta_o)}{\left[n(n+1)-\mu(\mu+1)\right]\left[m(m+1)-\mu(\mu+1)\right]} \left[\frac{dP^1}{d\theta}\bigg|_{\theta=\theta_o}\right]^2$$

$${}_d\psi^{nm}_\mu = i^{n+1} \frac{2n+1}{n(n+1)} \frac{j_n(kb)}{h_n(kb)} {}_d\xi^{nm}_\mu,$$

$${}_d\chi_n = i^{n+1} \frac{j'_n(kb)}{h'_n(kb)},$$

$${}_dK_n = \frac{n(n+1)}{(2n+1)}.$$

Each of the expressions (70) through (73) constitutes an infinite set of equations in an infinite number of unknowns for the particular coefficients involved, and the four expressions constitute the formal solution to the problem.

A few points about the solution are worthy of note. One may observe that in minimizing the mean square error in equation (49), the differentiation could have been carried out with respect to b_μ instead of d_m. This procedure, however, would result in a non-orthogonal integral over the range $0 - \theta_o$; furthermore, it would have necessitated the integration of the equations obtained from the magnetic field components over the range $0 - \pi$, and there exists no expansion for these components over the range $\theta_o - \pi$, thus making the integration impossible.

Also, although the finite energy condition at the tip was employed in the original selection of the functional expansion, the entire solution was obtained without the employment of the finite energy condition at the edge of the cone. The approximate treatments of Siegel[4,17] and Keller[18] predict that the major contribution to the scattered field arises from the singularity at the edge, and this viewpoint has been supported experimentally by the work of Keys and Primich[23], who found that the radar cross-sections of 60 and 120 degree finite cones correspond within 4 decibels ($db = 10 \log \frac{\sigma}{\lambda^2}$), σ = radar cross-section) to that of an annular wire ring of the same base diameter over a range of 0.5 - 3 wavelengths.

Since we know of no proof that the series of spherical harmonic functions used in this problem will properly display such an expected

singularity, the following section contains a numberical investigation of the field components in the vicinity of the edge for an interior apex angle of 30° (i.e., $\theta_o = 165°$).

Consideration of the arguments presented in Appendix B reveals that a singularity of permissible order occurs in all components of the magnetic field at the tip of the cone. No singularity occurs in the electric field at the tip.

Numerical Investigation of Singularities at the Edge

Since the edge singularities may easily be investigated by approaching the edge along a line in region II, only the expansion coefficients, c_n and d_n, of the scattered field in that region have been computed. Knowing these coefficients also enables one to compute the radar cross section and hence make a comparison with experimentally measured values. For convenience, the edge was approached along the line $\theta = \theta_o$, and since the Φ-variation is easily removed from all series summations, the actual computation was made for a particular field component divided by sin Φ or cos Φ, whichever was applicable. Consequently, any desired value of Φ may be inserted in the results.

Before proceeding with the numerical work, one must first choose particular values of cone angle and radius with which to work. In this case, our choices were primarily dictated by the information which is available.

To the best of the authors' knowledge, the most imformation available on the roots, μ and υ, of equations (32) and (34) is contained in part IV of the University of Michigan reports "Studies in Radar Cross

Sections" by Siegel, et.al.[16] This report evaluates the radar cross section for a semi-infinite cone and lists the first seven roots of each of the equations (32) and (34) for a cone angle $\theta_o = 165°$. Consequently, this angle was used in the following computations.

In addition to the data listed in the aforementioned report, the values of $P_\upsilon^1(\cos\theta_o)$ and $dP_\mu^1/d\theta\Big|_{\theta=\theta_o}$ were needed and have been computed (See Appendix C). For this computation, and throughout the analysis, the definition used for the associated Legendre function is

$$P_\upsilon^m(\cos\theta) = (-1)^m \frac{\Gamma(1+\upsilon+m)\sin^m\theta}{2^m\Gamma(1+\upsilon-m)\Gamma(1+m)} {}_2F_1\left(m-\upsilon, m+\upsilon+1; m+1; \frac{1-\cos\theta}{2}\right) \tag{74}$$

where ${}_2F_1$ is the ordinary hypergeometric function

$${}_2F_1(\alpha,\beta;\gamma;z) = F(\alpha,\beta;\gamma;z) = 1 + \frac{\alpha\beta}{1!}z + \frac{\alpha(\alpha+1)\beta(\beta+1)}{\gamma(\gamma+1)\ 2!}z^2 + \ldots; \tag{75}$$

and for the purposes of computing the derivative, the relation

$$\sin\theta \frac{dP_\upsilon^m}{d\theta} = (\upsilon-m+1)P_{\upsilon+1}^m(\cos\theta) - (\upsilon+1)\cos\theta\, P_\upsilon^m(\cos\theta) \tag{76}$$

was used. The roots given by Siegel and the computed values of the functions are listed in Table II.

At the present time, even less information seems to be available on the spherical Bessel and Hankel functions of non-integral order. As a result, a value of radius $kb = 0.1$ was chosen to facilitate approximation of the Bessel and Hankel functions by the first term in their series expansions. The approximations of the ratios of the Bessel functions listed in Table I are accurate to at least four significant figures for the value $\rho = kb = 0.1$. Though this value places our

TABLE I

BESSEL AND HANKEL FUNCTION APPROXIMATIONS

FOR $\rho \to 0$

$$j_\upsilon(\rho) \to \frac{\sqrt{\pi}}{2\Gamma(\upsilon+3/2)} \left(\frac{\rho}{2}\right)^{\upsilon} \qquad j_n(\rho) \to \frac{2^{2n} n!}{(2n+1)!} \left(\frac{\rho}{2}\right)^{n}$$

$$j'_\upsilon(\rho) \to \frac{\sqrt{\pi}\,(\upsilon+1)}{4\Gamma(\upsilon+3/2)} \left(\frac{\rho}{2}\right)^{\upsilon-1} \qquad j'_n(\rho) \to \frac{2^{2n-1}(n+1)!}{(2n+1)!} \left(\frac{\rho}{2}\right)^{n-1}$$

$$h_\upsilon(\rho) \to \frac{i\sqrt{\pi}}{2\sin(\upsilon+1/2)\pi\ \Gamma(-\upsilon+1/2)} \left(\frac{\rho}{2}\right)^{-(\upsilon+1)} \qquad h_n(\rho) \to \frac{i(2n)!}{2^{2n+1}\ n!} \left(\frac{\rho}{2}\right)^{-(n+1)}$$

$$h'_\upsilon(\rho) \to \frac{-i\sqrt{\pi}\ \upsilon}{\sin(\upsilon+1/2)\pi\ \Gamma(-\upsilon+1/2)} \left(\frac{\rho}{2}\right)^{-(\upsilon+2)} \qquad h'_n(\rho) \to \frac{-i(2n)!}{2^{2n+2}(n-1)!} \left(\frac{\rho}{2}\right)^{-(n+2)}$$

$$\frac{h'_n(\rho)}{h_m(\rho)} \frac{j_\upsilon(\rho)}{j'_\upsilon(\rho)} \to \frac{-m!(2n)!2^{2m-2n}}{(2m)!(n-1)!(\upsilon+1)} \left(\frac{\rho}{2}\right)^{m-n}$$

$$\frac{j'_n(\rho)}{h_m(\rho)} \frac{j_\upsilon(\rho)}{j'_\upsilon(\rho)} \to \frac{-im!(n+1)!2^{2m+2n+1}}{(2m)!(2n+1)!(\upsilon+1)} \left(\frac{\rho}{2}\right)^{n+m+1}$$

$$\frac{h_n(\rho)}{h'_m(\rho)} \frac{j'_\mu(\rho)}{j_\mu(\rho)} \to \frac{-(m-1)!(2n)!(\mu+1)2^{2m-2n}}{(2m)!n!} \left(\frac{\rho}{2}\right)^{m-n}$$

$$\frac{j_n(\rho)}{h'_m(\rho)} \frac{j'_\mu(\rho)}{j_\mu(\rho)} \to \frac{-i(m-1)!n!(\mu+1)2^{2m+2n-1}}{(2m)!(2n+1)!} \left(\frac{\rho}{2}\right)^{m+n+1}$$

$$-i^m \frac{(2m+1)}{m(m+1)} \frac{j_m(\rho)}{h_m(\rho)} \to \frac{i^{m+1}(m-1)!\,m!\ 2^{4m+1}}{[(2m)!]^2(m+1)} \left(\frac{\rho}{2}\right)^{2m+1}$$

$$i^{m+1} \frac{(2m+1)}{m(m+1)} \frac{j'_m(\rho)}{h'_m(\rho)} \to \frac{-i^m [(m-1)!]^2 2^{4m+1}}{[(2m)!]^2} \left(\frac{\rho}{2}\right)^{2m+1}$$

TABLE II

DATA USED IN COMPUTATION OF FIELD EXPANSION COEFFICIENTS

($\theta_o = 165°$)

n	$P_n^1(\cos\theta_o)$	$dP_n^1/d\theta\big\vert_{\theta=\theta_o}$	υ	$P_\upsilon^1(\cos\theta_o)$	B_υ	μ	$dP_\mu^1/d\theta\big\vert_{\theta=\theta_o}$	B_μ
1	-0.25881924	+0.96592579	0.9673	-0.52217	1.35806	1.03163	+1.88762	1.31078
2	+0.75000000	-2.5980742	1.9198	+1.40862	2.42491	2.08443	-5.17961	2.34637
3	-1.4228831	+4.3396881	2.8894	-2.28915	3.37945	3.14992	+9.50825	3.34731
4	+2.2069309	-5.4575812	3.8900	+2.98087	4.28564	4.22309	-14.65581	4.34068
5	-3.0177961	+5.1518426	4.9180	-3.50544	5.18033	5.30108	+20.49366	5.33248
6	+3.7646396	-2.6831313	5.9657	+3.92272	6.09038	6.38224	-26.92406	6.32433
7	-4.3581639	-2.5566144	7.0264	-4.27745	7.03236	7.46557	+34.15183	7.31653

$$B_\mu = \int_o^{\theta_o} [P_\mu^1(\cos\theta)]^2 \sin\theta\, d\theta; \quad B_\upsilon = \int_o^{\theta_o} [P_\upsilon^1(\cos\theta)]^2 \sin\theta\, d\theta.$$

NOTE: Values of μ and B_μ given by Ref. 16, Part IV, and computed by the Institute of Numberical Analysis, University of California.
Values of υ and B_υ given by Ref. 16, Part IV, and computed by Willow Run Research Center, University of Michigan.
Values of $P_\upsilon^1(\cos\theta_o)$ and $dP_\mu^1/d\theta\big\vert_{\theta=\theta_o}$ computed by School of Electrical Engineering, Purdue University.

computations well into the Rayleigh region (i.e., $b \approx \lambda/60$), it is satisfactory for investigation of the edge fields.

Using these apprdximations, the equations for the coefficients c_n and d_n, (72) and (73), may conveniently be broken into component parts and expressed as

$$\sum_n (\delta_m^n - a_{mn})c_n = B_m + K_m, \tag{77}$$

where

$$a_{mn} = F(m)G(n) \sum_\upsilon H(m,n,\upsilon),$$

$$F(m) = \frac{(2m+1)}{[m(m+1)]^2} \frac{2^{2m-1}m!}{(am)!} \left(\frac{\rho}{2}\right)^m,$$

$$G(n) = -\frac{n(n+1)}{2^{2n}} \frac{(2n)!}{(n-1)!} \left(\frac{\rho}{2}\right)^{-n},$$

$$H(m,n,\upsilon) = \frac{1}{(\upsilon+1)B_\upsilon} \frac{[\sin\theta_o P_\upsilon^1(\cos\theta_o)]^2}{[\upsilon(\upsilon+1)-m(m+1)][\upsilon(\upsilon+1)-n(n+1)]} \left[\frac{dP_m^1}{d\theta} \frac{dP_n^1}{d\theta}\right]_{\theta=\theta_o}$$

$$= \frac{\int_o^{\theta_o} P_\upsilon^1 P_m^1 \sin\theta \, d\theta \int_o^{\theta_o} P_\upsilon^1 P_n^1 \sin\theta \, d\theta}{(\upsilon+1) \int_o^{\theta_o} (P_\upsilon^1)^2 \sin\theta \, d\theta};$$

and

$$B_m = \sum_n -i^{n+1} b_{mn},$$

$$b_{mn} = -2^{4n+1} \left[\frac{(n-1)!}{(2n)!}\right]^2 \left(\frac{\rho}{2}\right)^{2n+1} a_{mn},$$

$$K_m = \frac{i^{m+1} 2^{4m+1}(m-1)!m!}{[(2m)!]^2 (m+1)} \left(\frac{\rho}{2}\right)^{2m+1};$$

for equation (72), and for (73),

$$\sum_n (\delta_m^n - f_{mn})\, d_n = G_m + K'_m \,, \tag{78}$$

where

$$I(m) = \frac{(2m+1)}{[m(m+1)]^2} \frac{2^{2m-1}(m-1)!}{(2m)!} \left(\frac{\rho}{2}\right)^m \,,$$

$$J(n) = -\frac{n(n+1)}{2^n} \frac{(2n)!}{n!} \left(\frac{\rho}{2}\right)^{-n} \,,$$

$$K(m,n,\mu) = \frac{(\mu+1)}{B_\mu} \frac{\sin^2\theta_o P_n^1(\cos\theta) P_m^1(\cos\theta)}{[n(n+1)-\mu(\mu+1)][n(n+1)-\mu(\mu+1)]} \left[\frac{dP^1}{d\theta}\right]^2_{\theta=\theta_o}$$

$$= (\mu+1) \frac{\int_o^{\theta_o} P_\mu^1 P_n^1 \sin\theta\, d\theta \int_o^{\theta_o} P_\mu^1 P_m^1 \sin\theta\, d\theta}{\int_o^{\theta_o} (P_\mu^1)^2 \sin\theta\, d\theta} \,;$$

and

$$G_m = \sum_n i^n g_{mn},$$

$$g_{mn} = -2^{4n+1} \frac{n!(n-1)!}{(n+1)[(2n)!]^2} \left(\frac{\rho}{2}\right)^{2n+1} f_{mn} \,,$$

$$K'_m = -i^m 2^{4m+1} \left[\frac{(m-1)!}{(2m)!}\right]^2 \left(\frac{\rho}{2}\right)^{2m+1} \,.$$

Equations (77) and (78) each represent one equation; however, by letting m assume successive integral values, one obtains a set of equations for each representation. Let (x_{mn}) represent the element of a matrix in the m^{th} row and the n^{th} column, and let $[x_{mn}]$ represent the matrix formed by these elements. Then the set of equations represented by (77) and (78) may be represented in matrix form as

$$[\delta_m^n - a_{mn}]\,[c_n] = [B_m + K_m], \tag{79}$$

$$[\delta_m^n - f_{mn}]\,[d_n] = [G_m + K'_m], \tag{80}$$

respectively.

Throughout the computations, summations over seven terms were used. The expanded 7 x 7 matrices are shown in Table III, and the computed matrix coefficients are listed in Table IV.

Utilizing these matrix coefficients, the electromagnetic field expansion coefficients, c_n and d_n, were repeatedly computed using sets of seven, six, five, four, and three equations by successively eliminating the last row and column of the matrices. Thus, by comparing the solutions listed in Table V, an estimate of the degree of accuracy may be obtained. In every case the magnitudes of the coefficients computed using three equations lie within two per-cent of the magnitudes of those computed using seven equations. Also, an examination of $|c_1/c_2|$ and $|d_1/d_2|$ yields factors of 200 and 140, respectively, indicating very rapid convergence of the series, as may be expected for such a small value of kb.

Having obtained the field expansion coefficients, we were thus finally prepared to return to equations (17) and (27) for computation of the field components. For this purpose, each field component was separated into its real and imaginary parts. Since

$$h_n(\rho) = j_n(\rho) - in_n(\rho), \tag{81}$$

and

$$n_n(\rho) = (-1)^{n+1} j_{-n}(\rho); \tag{82}$$

if we let

$$k_n(\rho) = (-1)^n j_{-n}(\rho), \tag{83}$$

TABLE III

MATRIX FORM OF EXPANSION COEFFICIENT EQUATIONS

$$\begin{bmatrix} (1-a_{11}) & -a_{12} & -a_{13} & -a_{14} & -a_{15} & -a_{16} & -a_{17} \\ -a_{21} & (1-a_{22}) & -a_{23} & -a_{24} & -a_{25} & -a_{26} & -a_{27} \\ -a_{31} & -a_{32} & (1-a_{33}) & -a_{34} & -a_{35} & -a_{36} & -a_{37} \\ -a_{41} & -a_{42} & -a_{43} & (1-a_{44}) & -a_{45} & -a_{46} & -a_{47} \\ -a_{51} & -a_{52} & -a_{53} & -a_{54} & (1-a_{55}) & -a_{56} & -a_{57} \\ -a_{61} & -a_{62} & -a_{63} & -a_{64} & -a_{65} & (1-a_{66}) & -a_{67} \\ -a_{71} & -a_{72} & -a_{73} & -a_{74} & -a_{75} & -a_{76} & (1-a_{77}) \end{bmatrix} \begin{bmatrix} c_1 \\ c_2 \\ c_3 \\ c_4 \\ c_5 \\ c_6 \\ c_7 \end{bmatrix} = \begin{bmatrix} B_1+K_1 \\ B_2+K_2 \\ B_3+K_3 \\ B_4+K_4 \\ B_5+K_5 \\ B_6+K_6 \\ B_7+K_7 \end{bmatrix}$$

$$\begin{bmatrix} (1-f_{11}) & -f_{12} & -f_{13} & -f_{14} & -f_{15} & -f_{16} & -f_{17} \\ -f_{21} & (1-f_{22}) & -f_{23} & -f_{24} & -f_{25} & -f_{26} & -f_{27} \\ -f_{31} & -f_{32} & (1-f_{33}) & -f_{34} & -f_{35} & -f_{36} & -f_{37} \\ -f_{41} & -f_{42} & -f_{43} & (1-f_{44}) & -f_{45} & -f_{46} & -f_{47} \\ -f_{51} & -f_{52} & -f_{53} & -f_{54} & (1-f_{55}) & -f_{56} & -f_{57} \\ -f_{61} & -f_{62} & -f_{63} & -f_{64} & -f_{65} & (1-f_{66}) & -f_{67} \\ -f_{71} & -f_{72} & -f_{73} & -f_{74} & -f_{75} & -f_{76} & (1-f_{77}) \end{bmatrix} \begin{bmatrix} d_1 \\ d_2 \\ d_3 \\ d_4 \\ d_5 \\ d_6 \\ d_7 \end{bmatrix} = \begin{bmatrix} G_1+K_1' \\ G_2+K_2' \\ G_3+K_3' \\ G_4+K_4' \\ G_5+K_5' \\ G_6+K_6' \\ G_6+K_7' \end{bmatrix}$$

TABLE IV

COMPUTED MATRIX COEFFICIENTS

$\delta_m^n = \begin{cases} 0, & m \neq n \\ 1, & m = n \end{cases}$ $\quad (\delta_m^n - a_{nm}) = A \times 10^p$ $\quad (\delta_m^n - f_{nm}) = F \times 10^q$

m	n	A	p	F	q
1	1	.15094515	+1	.30369545	+1
1	2	-.16087902	+1	-.65378349	+1
1	3	.22875915	+3	.86326182	+3
1	4	-.27292641	+5	-.10182327	+6
1	5	.25126402	+7	.99152403	+7
1	6	-.43697134	+7	-.21936376	+9
1	7	-.98911438	+11	-.34144258	+12
2	1	-.55171124	-4	-.22420560	-3
2	2	.16874330	+1	.25430143	+1
2	3	-.18685502	+1	-.54724578	+1
2	4	.20854942	+3	.59734267	+3
2	5	-.13911531	+5	-.41698784	+5
2	6	-.21496838	+7	-.57300361	+7
2	7	.14642109	+10	.44408800	+10
3	1	.36609829	-6	.13815346	-5
3	2	-.87199009	-4	-.25538139	-3
3	3	.17783107	+1	.23657812	+1
3	4	-.10617697	+1	-.26795574	+1
3	5	-.10066070	+2	-.47242174	+2
3	6	.43267581	+5	.12306150	+6
3	7	-.17732992	+8	-.53186446	+8
4	1	-.18566424	-8	-.69267537	-8
4	2	.41369394	-6	.11849328	-5
4	3	-.45132954	-4	-.11390072	-3
4	4	.18190171	+1	.22521805	+1
4	5	.12758369	+1	.36978912	+1
4	6	-.53985136	+3	-.15565716	+4
4	7	.17443197	+6	.53260609	+6
5	1	.61135626	-11	.24124998	-10
5	2	-.98702126	-9	-.29585232	-8
5	3	-.15303994	-7	-.71824845	-7
5	4	.45632737	-4	.13226212	-3
5	5	.18287685	+1	.21528669	+1
5	6	.50559947	+1	.14933190	+2
5	7	-.14279264	+4	-.45071280	+4
6	1	-.31536749	-15	-.15831749	-13
6	2	-.45240369	-11	-.12058933	-10
6	3	.19512248	-8	.55496672	-8
6	4	-.57273732	-6	-.16513928	-5
6	5	.14997075	-3	.44294782	-3
6	6	.18237081	+1	.20498085	+1
6	7	.99545654	+1	.33061918	+2

TABLE IV

$$\delta_m^n = \begin{cases} 0, & m \neq n \\ 1, & m = n \end{cases} \qquad (\delta_m^n - a_{nm}) = A \times 10^p \qquad (\delta_m^n - f_{nm}) = F \times 10^q$$

m	n	A	p	F	q
7	1	-.17624170	-15	-.60838698	-15
7	2	.76076983	-13	.23073779	-12
7	3	-.19743535	-10	-.59216661	-10
7	4	.45688357	-8	.13950367	-7
7	5	-.10456922	-5	-.33006392	-5
7	6	.2457652	-3	.81625573	-3
7	7	.18467407	+1	.19255892	+1

m	$G_m + K_m^0$	$B_m + K_m$
1	.12102484[-5] + i.18445300[-4]	.94402300[-5]-i.44673140[-6]
2	-.79629000[-8]-i.11190013[-6]	-.55078856[-7]+i.57672100[-8]
3	.4047280693[-10]+i.68956550[-9]	.36470023[-9]-i.23215924[-10]
4	-.3821715450[-12]-i.34591569[-11]	-.18544132[-11]+i.11480715[-12]
5	.54847416[-15]+i.12065140[-13]	.61143160[-14]-i.27443110[-15]
6	.22256242[-17]-i.81212522[-17]	-.41165708[-18]-i.12534308[-17]
7	-.42665968[-19]-i.30200151[-18]	-.17526716[-18]+i.21106598[-19]

TABLE V

EXPANSION COEFFICIENTS OF THE ELECTROMAGNETIC FIELD

$c_n = (x)[-p] = x\ 10^{-p}$

*	c_1	c_2	c_3	c_4
7x7	(6.160-i0.288)[-6]	(-3.199+i0.337)[-8]	(2.008-i0.132)[-10]	(-9.951+i0.606)[-13]
6x6	(6.166-i0.289)	(-3.207+i0.338)	(2.017-i0.133)	(-10.04+i0.616)
5x5	(6.166-i0.289)	(-3.206+i0.338)	(2.017-i0.134)	(-10.03+i0.618)
4x4	(6.171-i0.289)	(-3.209+i0.339)	(2.016-i0.134)	(-10.01+i0.617)
3x3	(6.189-i0.290)	(-3.221+i0.339)	(2.022-i0.134)	

*	c_5	c_6	c_7
7x7	(3.266-i0.138)[-15]	(-6.281-i6.994)[-19]	(-8.646+i1.099)[-20]
6x6	(3.335-i0.147)	(-11.09-i6.332)	
5x5	(3.332-i0.149)		

$d_n = (y)[-q] = y\ 10^{-q}$

*	d_1	d_2	d_3	d_4
7x7	(0.381+i5.823)[-6]	(-0.299-i4.226)[-8]	(0.188+i2.796[-10]	(-0.087-i1.466)[-12]
6x6	(0.383+i5.833)	(-0.303-i4.245)	(0.193+i2.823)	(-0.093-i1.496)
5x5	(0.382+i5.834)	(-0.303-i4.244)	(0.193+i2.819)	(-0.093-i1.491)
4x4	(0.383+i5.852)	(-0.303-i4.253)	(0.193+i2.818)	(-0.093-i1.481)
3x3	(0.386+i5.901)	(-0.306-i4.287)	(0.194+i2.834)	

*	d_5	d_6	d_7
7x7	(0.201+i5.368)[-15]	(1.239-i5.340)[-18]	(-0.206-i1.193)[-19]
6x6	(0.246+i5.633)	(0.891-i7.353)	
5x5	(0.253+i5.582)		

* Size of Matrix

the Hankel function becomes

$$h_n(\rho) = j_n(\rho) + ik_n(\rho). \tag{84}$$

Using this notation, one obtains from (27)

$$\mathrm{Re}(E_r) = \cos\phi \sum_n \frac{n(n+1)}{\rho} \left[d_n^r j_n(\rho) - d_n^i k_n(\rho)\right] P_n^1(\cos\theta) \tag{85}$$

$$\mathrm{Im}(E_r) = \cos\phi \sum_n \frac{n(n+1)}{\rho} \left[d_n^i j_n(\rho) + d_n^r k_n(\rho)\right] P_n^1(\cos\theta) \tag{86}$$

$$\mathrm{Re}(E_\theta) = \cos\phi \sum_n \left\{ \left[c_n^r j_n(\rho) - c_n^i k_n(\rho)\right] \frac{P_n^1(\cos\theta)}{\sin\theta} + \left[d_n^r j_n'(\rho) - d_n^i k_n'(\rho)\right] \frac{dP_n^1}{d\theta} \right\} \tag{87}$$

$$\mathrm{Im}(E_\theta) = \cos\phi \sum_n \left\{ \left[c_n^i j_n(\rho) + c_n^r k_n(\rho)\right] \frac{P_n^1(\cos\theta)}{\sin\theta} + \left[d_n^i j_n'(\rho) + d_n^r k_n'(\rho)\right] \frac{dP_n^1}{d\theta} \right\} \tag{88}$$

$$\mathrm{Re}(E_\phi) = -\sin\phi \sum_n \left\{ \left[c_n^r j_n(\rho) - c_n^i k_n(\rho)\right] \frac{dP_n^1}{d\theta} + \left[d_n^r j_n'(\rho) - d_n^i k_n'(\rho)\right] \frac{P_n^1(\cos\theta)}{\sin\theta} \right\} \tag{89}$$

$$\mathrm{Im}(E_\phi) = -\sin\phi \sum_n \left\{ \left[c_n^i j_n(\rho) + c_n^r k_n(\rho)\right] \frac{dP_n^1}{d\theta} + \left[d_n^i j_n'(\rho) + d_n^r k_n'(\rho)\right] \frac{P_n^1(\cos\theta)}{\sin\theta} \right\} \tag{90}$$

where $\rho = kr$, $c_n = c_n^r + ic_n^i$ and $d_n = d_n^r + id_n^i$; the superscripts 'r' and 'i' representing the real and imaginary parts, respectively. For the computation of the field components, only spherical Bessel functions of integral order were needed, and for these functions, data are readily available (Ref. 27).

The results of these computations are listed in Table VI and are illustrated in figures 4 and 5. Although one could not expect to obtain a true singularity at the edge of the cone by using only a finite number of terms, figure 4 clearly indicates that the spherical harmonic functions used in the field expansions do represent the edge singularity. Furthermore, not only does the singularity lie well within the $(kR)^{-1}$ limit imposed

COMPONENTS OF THE SCATTERED ELECTRIC FIELD NEAR THE EDGE OF A FINITE CONE

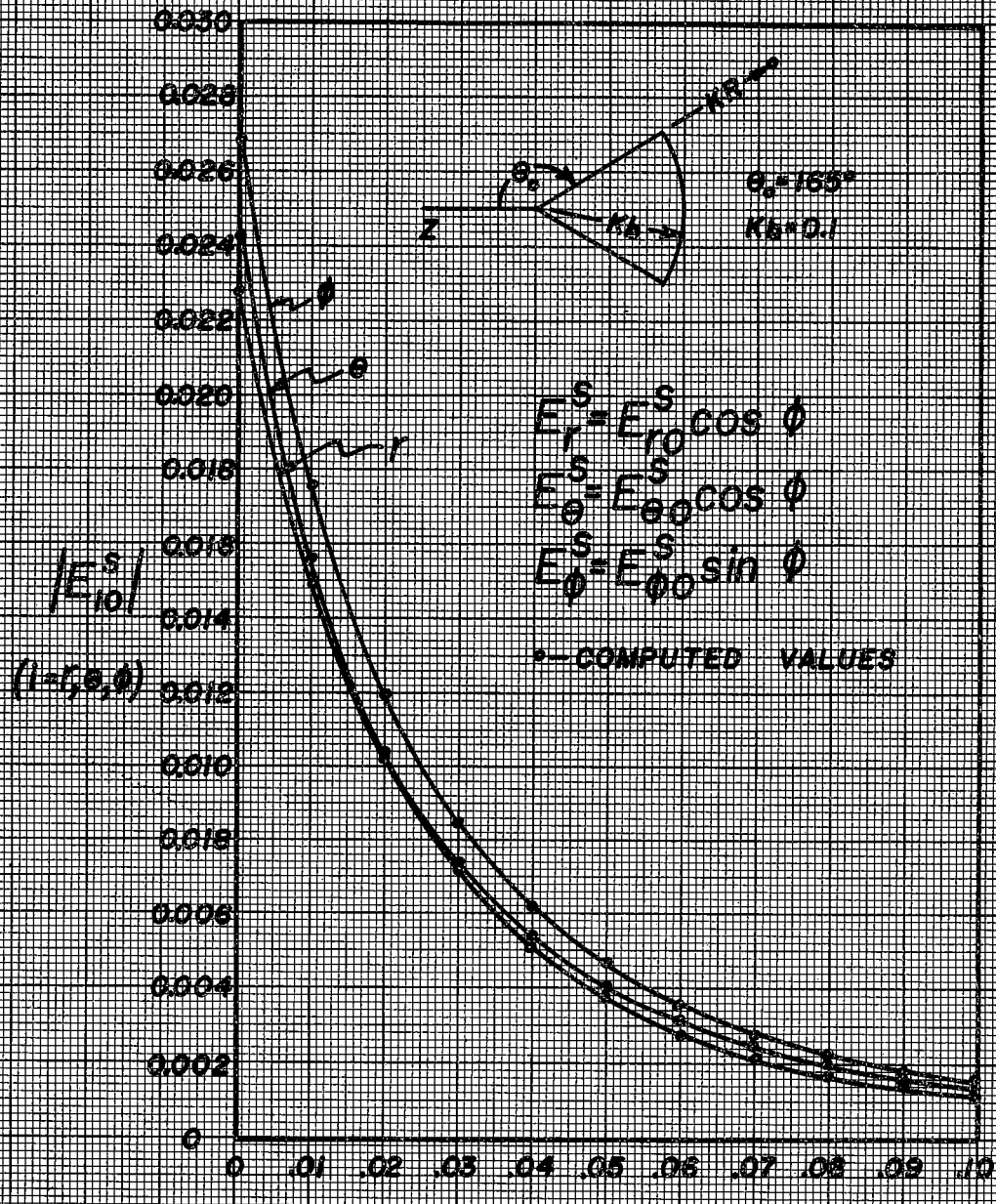

Figure 4

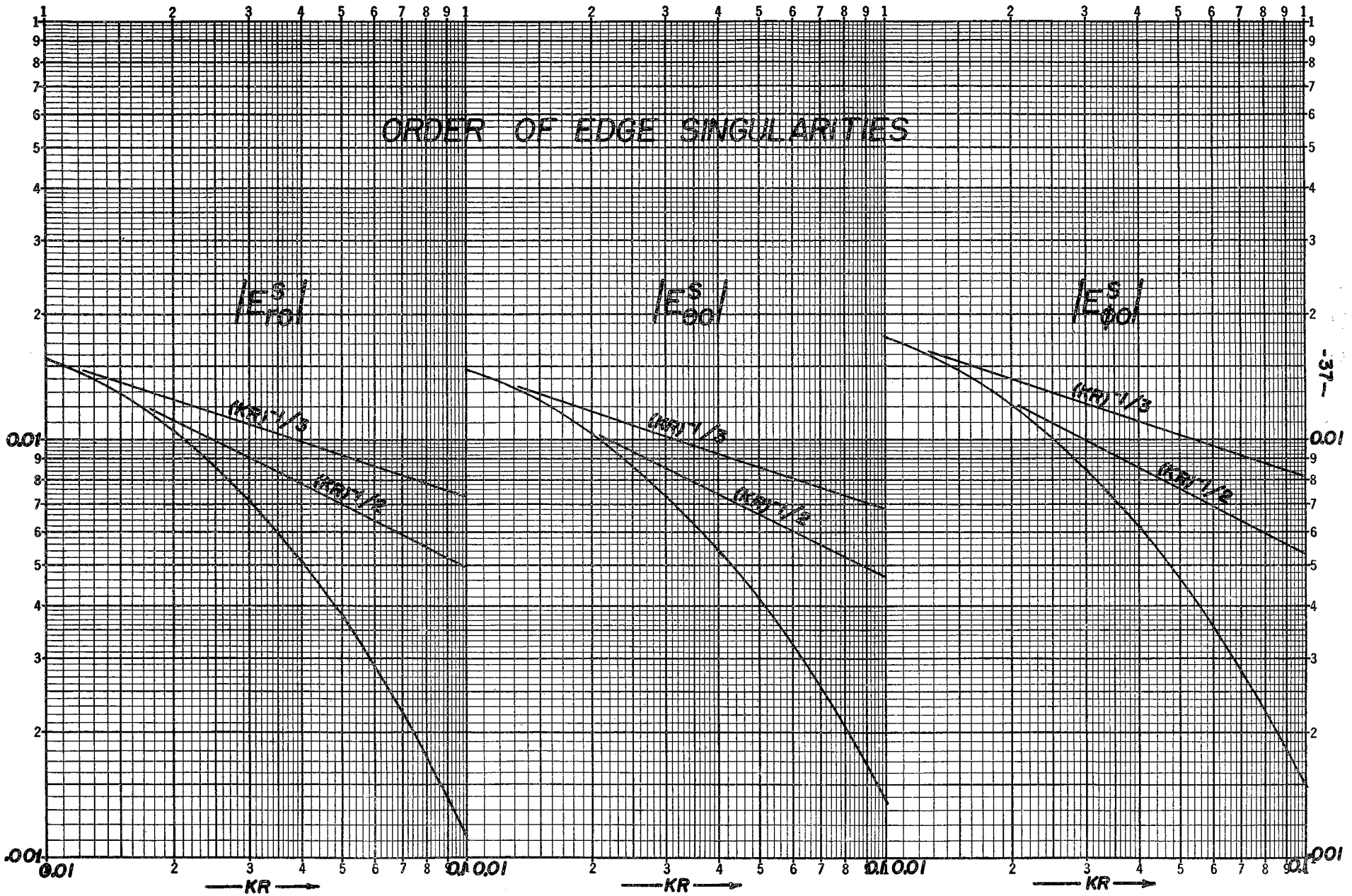
ORDER OF EDGE SINGULARITIES
$|E^s_{r01}|$
$|E^s_{\theta 01}|$
$|E^s_{\phi 01}|$
$(KR)^{-1/3}$
$(KR)^{-1/2}$
KR
0.01
0.1
0.001

FIGURE 5

TABLE VI

ELECTRIC FIELD COMPONENTS NEAR THE EDGE OF A FINITE CONE

kR	E_{ro}	$\lvert E_{ro}\rvert$	$E_{\theta o}$	$\lvert E_{\theta o}\rvert$	$E_{\phi o}$	$\lvert E_{\phi o}\rvert$
0.00	(2.42-i0.07)	2.43	2.26-i0.26	2.28	-2.68+i0.24	2.69
0.01	(1.56-i0.07)	1.56	1.48-i0.19	1.49	-1.75+i0.18	1.76
0.02	(1.03-i0.05)	1.04	1.01-i0.14	1.02	-1.20+i0.14	1.20
0.03	(0.72-i0.04)	0.72	0.72-i0.11	0.73	-0.85+i0.10	0.85
0.04	(0.51-i0.03)	0.51	0.53-i0.08	0.54	-0.62+i0.08	0.62
0.05	(0.38-i0.02)	0.38	0.40-i0.07	0.41	-0.47+i0.07	0.47
0.06	(0.28-i0.02)	0.28	0.31-i0.06	0.32	-0.36+i0.06	0.36
0.07	(0.22-i0.01)	0.22	0.24-i0.05	0.25	-0.28+i0.05	0.28
0.08	(0.17-i0.01)	0.17	0.20-i0.04	0.20	-0.22+i0.04	0.23
0.09	(0.14-i0.01)	0.14	0.16-i0.03	0.16	-0.18+i0.03	0.18
0.10	(0.11-i0.01)	0.11	0.13-i0.03	0.14	-0.15+i0.03	0.15

kR = distance from edge at $\theta = \theta_o = 165°$

$E_r = E_{ro} \cos \phi \times 10^{-2}$

$E_\theta = E_{\theta o} \cos \phi \times 10^{-2}$

$E_\phi = E_{\phi o} \sin \phi \times 10^{-2}$

by the finite energy condition, but it closely approximates the $(kR)^{-(1/3)}$ singularity which would be predicted from the considerations presented in Appendix B for a 90° edge. It is interesting to note that in a check computation using a desk calculator, six of the first seven terms in the expansion of $Re(E_r)$ added up in phase, and that each of the terms was of the same order of magnitude, indicating that the series was diverging at that point.

Consideration of the results of appendix B reveals that similar singularities will also occur in the magnetic field components.

Radar Cross Section

Within recent years, a few experimental measurements of the radar cross section of finite cones have been made, thus providing an experimental check on our theoretical results. The radar cross section, σ, is defined to be

$$\sigma = 4\pi r^2 \lim_{r\to\infty} \frac{\bar{S}^s_{II}}{\bar{S}^i_{II}}, \tag{91}$$

where $\bar{S} = \frac{1}{2} Re(\bar{E} \times \bar{H}^*)$, the average Poynting vector ($\bar{H}^*$ represents the complex conjugate of $\bar{H}$). For the coordinate system with which we have been concerned (figure 1), the radar cross section, when evaluated for $\theta = 0$, is more precisely termed the back-scattering radar cross section. Herein, we have concerned ourselves with only this case, although the fact will not be explicitely mentioned with each reference to the cross section.

From equations (74) and (75), it may be seen that

$$\left.\frac{P_n^1(\cos\theta)}{\sin\theta}\right|_{\theta=0} = \left.\frac{dP_n^1}{d\theta}\right|_{\theta=0} = \frac{-n(n+1)}{2}, \tag{92}$$

and the limiting form of the Hankel function and its derivative are

$$h_n(\rho) \underset{\rho\to\infty}{\to} \frac{i^{n+1}}{\rho} e^{-i\rho}, \tag{93}$$

$$h_n'(\rho) = \frac{1}{\rho}\frac{d}{d\rho}[\rho h_n(\rho)] \underset{\rho\to\infty}{\to} \frac{i^n}{\rho} e^{-i\rho}. \tag{94}$$

Noticing that the present case, $\bar{S}_{II}^{i} = 1/2\eta$, and utilizing the above relations in equations (17) and (24), the radar cross section may be expressed (after some algebra),

$$\sigma = \frac{\lambda^2}{4\pi}\left|\sum_n i^n\, n(n+1)\,(c_n - id_n)\right|^2. \tag{95}$$

Utilizing the coefficients listed in table V, one obtains

$$\sigma = 0.459 \times 10^{-10}\,\lambda^2.$$

Siegel[4] has postulated that the cross section of any body of revolution in the Rayleigh region may be expressed as

$$\sigma = \frac{4}{\pi} k^4 V^2 \left(1 + \frac{e^{-y}}{\pi y}\right)^2, \tag{96}$$

where $k = 2\pi/\lambda$, V = volume of the body, and for a finite cone, $y = h/4r$ (h = height of cone, r = radius of base). For a 30° cone with $kb = 0.1$ ($b = h/\cos 15°$), this result yields

$$\sigma = 1.875 \times 10^{-10}\,\lambda^2,$$

which is greater than our results by a factor of 4.1.

The authors know of no measurements which have been made on finite

cones of such small cross section, however, Brysk, Hiatt, Weston, and Siegel[28] have approached the Rayleigh region with a finite cone of 24°. Their results are shown in figure 6. The Rayleigh line shown is approximately

$$\frac{\sigma}{\pi r^2} = 12\,(2\pi n)^4 \tag{97}$$

where $n = r/\lambda$, r = radius of the base. Using (96) to predict the ratio between a 24° and a 30° finite cone of the same base radius, one obtains

$$\sigma_{12°} = 1.47\,\sigma_{15°} \tag{98}$$

From (97) and (98), one may predict the cross section of the 30° finite cone to be

$$\sigma = 1.949 \times 10^{-10}\,\lambda^2,$$

this value being approximately 4.2 times that obtained by (95).

A comparison with the radar cross section of a sphere, given by

$$\frac{\sigma}{\pi r^2} = 1.403\,(r/\lambda)^4 \times 10^4 \tag{99(}$$

(Ref. 29, p. 452), was also made by finding the ratio of the cross section of a sphere to that of a cone of the same volume for the cases of the 30° cone and the experimental measurements of figure 6. These results also indicate that the cross section computed from (95) using the data listed in table II is low by a factor of approximately four.

Investigation of (95) and (77) reveals that the cross section of the case under consideration is predominantly determined by the coefficient c_1, which is in turn predominately determined by the equation

$$(1 - a_{11})\,c_1 = (-a_{11} - 0.5) \times 10^{-3}. \tag{100}$$

EXPERIMENTAL MEASUREMENT OF THE
RADAR CROSS SECTION OF A FINITE CONE

FROM BRYSK, HIATT, WESTON, & SIEGEL
"THE NOSE-ON RADAR CROSS SECTIONS OF FINITE CONES"
CANADIAN JOURNAL OF PHYSICS, VOL. 37, 1959

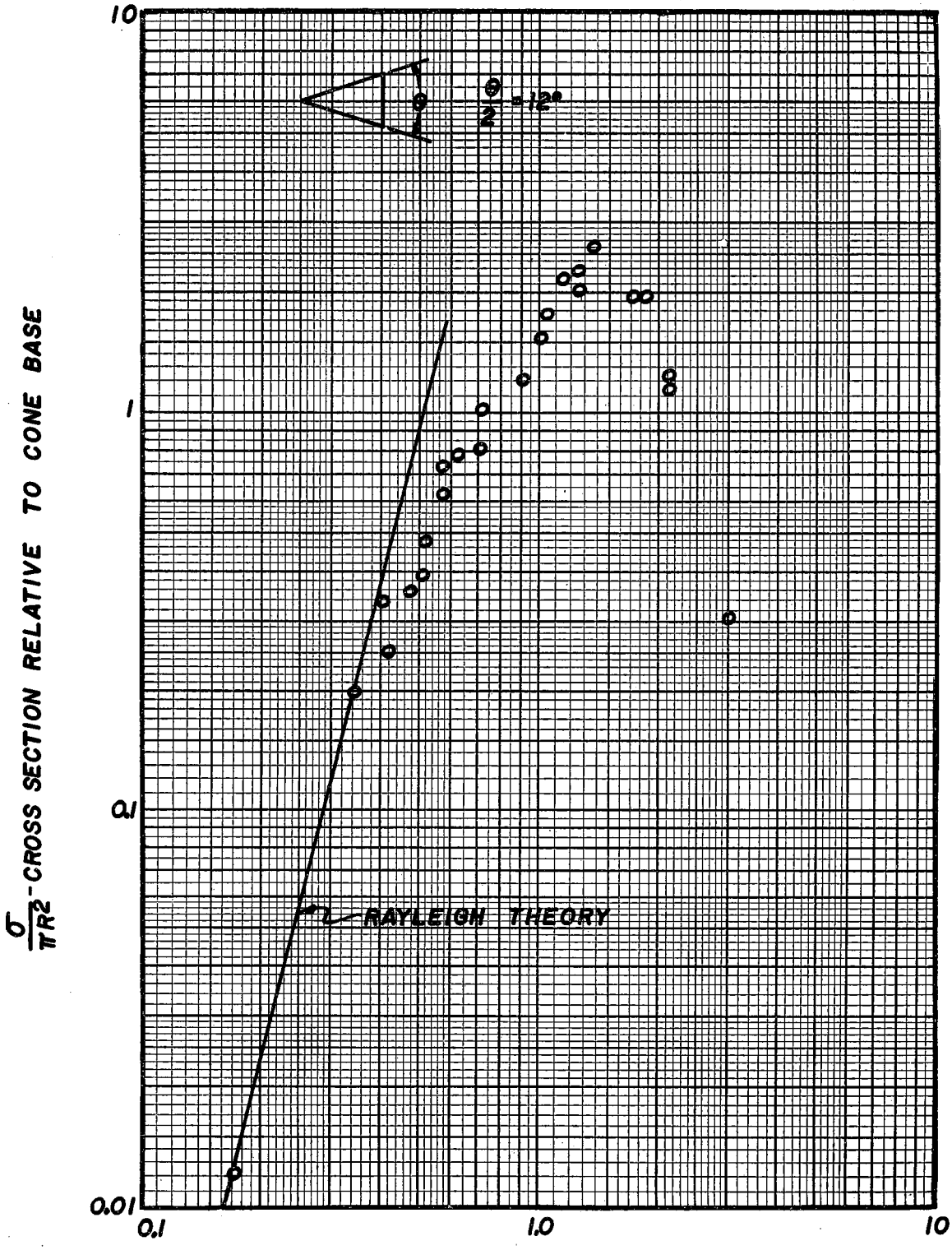

Figure 6

where $a_{11} = -0.50945154$. This equation, as well as all terms of (79) and (80) are very sensitive to the precise value of υ.

Siegel[16] has also noted this sensitivity in the computation of the cross section of a semi-infinite cone from the Hansen and Schiff solution. Although two computations for the values of υ are not available for comparison, a comparison of the first four values of μ are computed by the University of Michigan and the University of California is as follows:

U of M	U of C	Difference
1.03158	1.03163	.00005
2.08631	2.08443	.00082
3.14588	3.14992	.00404
4.21990	4.22309	.00319.

The authors of Ref. 16 further note that the California results are the more accurate.

Further investigation of (100) reveals that if the first root, $\upsilon_1 = 0.9673$, were larger by an amount 0.0003, the radar cross section would increase by a factor of four. Consequently, knowledge of the roots of (32) and (34) to at least six decimal places seems to be an absolute necessity if one is to accurately compute the radar cross section for such small cone angles. Since the more accurate computations for the first four values of μ are in each case higher than the approximate computation, the result predicted using (95) should be somewhat low if accurate values of υ are also higher than those used in the computation.

In view of these facts, it is believed that the foregoing results are as accurate as can be reasonably expected with the data that are presently available.

Summary and Conclusions

An exact solution to the scattering of a plane electromagnetic wave by a finite cone has been obtained using a relatively straightforward procedure. It is believed that the techniques used herein may be further applied to aid in obtaining exact solutions for other irregularly-shaped scatterers whose surfaces are not described by fixing only one coordinate. Although the numerical computation of results form the solution is not simple, it is also certainly not prohibitive with modern digital computers, and the ability to obtain numerical results for the "resonance" region is only hindered by the lack of functional data of well-known functions.

The singularities which may occur in electromagnetic fields have also been investigated, and their theoretical existence using vector solutions of the wave equation has been demonstrated.

It is intended that work on other irregularly-shaped objects will continue, as well as the further computation of necessary functional data for use in obtaining more precise and extended results from the present solution.

LIST OF REFERENCES

1. Lord Rayleigh, "Incidence of Aerial and Electric Waves on Small Obstacles," Phil. Mag., 44 (1897) 28.

2. Fock, V. A., "The Field of a Plane Wave Near the Surface of a Conducting Body," J. Physics, USSR, 10 (1946) 399; also "Diffraction, Refraction, and Reflection of Radio Waves," 13 papers by V. A. Fock, ASTIA Document No. AD117276.

3. Stratton, J. A., Electromagnetic Theory, McGraw-Hill, 1941.

4. Siegel, K. M., "Far Field Scattering from Bodies of Revolution," Appl. Sci. Res., B7 (1959) 293.

5. Seitz, W., "Die Wirkung eines unendlich langen Metallzylinder auf Hertzsche Wellen," Ann. d. Phys., 16 (1905) 746.

6. Ignatowsky, W. V., "Reflexion electromagnetischer Wellen an einem Draht," Ann. d. Phys., 18 (1905) 495.

7. Sommerfeld, A., "On the Mathematical Theory of Diffraction," Math. Ann., 47 (1896) 317.

8. Oberhettinger, F., "Diffraction of Waves by a Wedge," Comm. Pure App. Math., 7 (1954) 551.

9. Hansen, W. W., and L. I. Schiff, "Theoretical Study of Electromagnetic Waves Scattered from Shaped Metal Surfaces," Quarterly Report No. 4, Stanford University Microwave Laboratory, (1948).

10. Horton, C. W., and F. C. Karal, Jr., "Diffraction of a Plane Electromagnetic Wave by a Paraboloid of Revolution," J. App. Phys., 22-5 (1951) 575.

11. Mie, G., "Beitrage zur Optik truber Medien special kolloidaler Metallesungen," Ann. d. Phys., 25 (1908) 377.

12. Schultz, F. V., "Scattering by a Prolate Spheroid," Studies in Radar Cross Sections I, UMM-42, Willow Run Research Center, University of Michigan (1950).

13. Moglich, F., "Diffraction Phenomena at Bodies of Elliptical Shape," Ann. d. Phys., 83 (1927) 609.

14. Spence, R. D. and A. Leitner, "Diffraction of Circular Disks and Apertures," Phys. Rev., 74 (1948) 349.

15. Meixner, J., "Strenge Theorie der Beugung electromagentischer Wellen an der vollkommen leitenden Kreisscheibe," Zeit. f. Naturforschung, 3a (1948) 506.

16. Siegel, K. M., et al, "Studies in Radar Cross Sections II, III, and IV," UMM 82, 87, 92, Willow Run Research Center, University of Michigan, (1951-52-53).

17. Siegel, K. M., R. F. Goodrich, and V. H. Weston, "Comments on Far Field Scattering from Bodies of Revolution," Appl. Sci. Res., 8B (1959) 8.

18. Keller, J. B., "Backscattering from a Finite Cone," IRE Trans. on Ant. and Prop., AP-8 (1960) 175.

19. Sommerfeld, A., Optics, (Vol. IV, Lectures on Theoretical Physics), Academic Press, Inc., (1949), p. 249.

20. Schelkunoff, S. A., Advanced Antenna Theory, John Wiley and Sons, (1952).

21. Sommerfeld, A., Partial Differential Equations in Physics, (Vol. VI, Lectures on Theoretical Physics), Academic Press Inc., (1949).

22. Schelkunoff, S. A., Applied Mathematics for Engineers and Scientists, D. Van Nostrand, (1948).

23. Keys, J. E., and R. I. Primich, "The Experimental Determination of the Far-Field Scattering from Simple Shapes," Defence Research Tele-communications Establishment, Defence Research Board, Canada, also Can. J. Phys., 37 (1959) 521.

24. Hobson, E. W., The Theory of Spherical and Ellipsoidal Harmonics, Chelsea Publishing Co., (1955); Cambridge University Press, (1931).

25. Morse, P. M., and H. Feshbach, Methods of Theoretical Physics, McGraw-Hill, (1953).

26. Meixner, Josef, "The Behavior of Electromagnetic Fields at Edges," New York University, Research Report No. EM-72, (1954).

27. Mathematical Tables Project, National Bureau of Standards, Tables of Spherical Bessel Functions, Columbia University Press, (1947).

28. Brysk, H., R. E. Hiatt, V. H. Weston, and K. M. Siegel, "The Nose-On Radar Cross Section of Finite Cones," Canadian Journal of Physics, 37 (1959) 675.

29. Kerr, D. E., Propagation of Short Radio Waves, Radiation Laboratory Series, MIT, Vol. 13. McGraw-Hill, (1951).

30. Whittaker, E. T., and G. N. Watson, A Course in Modern Analysis, Cambridge University Press, (1952), Original Edition (1902).

31. Magnus, W., and F. Oberhettinger, Functions of Mathematical Physics, Chelsea Publishing Co., (1954).

32. Erdelyi, Magnus, Oberhettinger, Tricomi, Higher Transcendental Functions, Bateman Manuscript Project Vol. I and II, California Institute of Technology, McGraw-Hill, (1953),

33. Muller, Claus, Grundprobleme der mathematischen Theorie electromagnetischer Schwingungen, Springer-Verlag, Berlin, (1957).

34. Centre National D'Études des Télécommunications, "Tables des Fonctions de Legendre Associées," Éditions de la Revue D' Optique, (1952).

35. Franz, W., and K. Depperman, "Theorie der Beugung am Zylinder unter Beruckschtigung der Kriechwelle," Ann. d. Phys., 10 (1952) 361.

APPENDIX A

SELECTION OF ORTHOGONAL FUNCTIONS

For mathematical solutions of the type which we are concerned, it is always desirable that the unknown expansion coefficients be finally determined, rather than appearing in a set of an infinite number of equations. In the latter case, the value obtained for an expansion coefficient depends on the number of equations used in the solution, whereas coefficients which possess finality may be determined explicitly and exactly from a single equation without the use of a set of equations involving several unknowns.

For such a finality, however, it becomes necessary to obtain orthogonal expansions for the fields on each side of a matching boundary. For instance, in the case illustrated by figure 3, the expansions in both regions I and II must be orthogonal over the range $\theta = 0 \rightarrow \theta_o$ when matching the fields across the imaginary spherical boundary, $r = b$. Also, the field expansions in regions II and III must be orthogonal over the range $r = b \rightarrow \infty$ when matching the fields across the imaginary conical boundary, $\theta = \theta_o$.

Although such an orthogonalization may still present numerous questions, it seems that the proper selection of the degree, τ, of the associated Legendre functions will produce functions orthogonal to both r and θ for the configuration shown in figure 3.

To show this, consider the associated Legendre equations of degree τ and τ', respectively:

$$\frac{d}{d\theta}\left(\sin\theta \frac{dP^m_\tau}{d\theta}\right) = \left[-\tau(\tau+1)\sin\theta + \frac{m^2}{\sin\theta} \right] P^m_\tau \qquad \text{(A-1)}$$

$$\frac{d}{d\theta}\left(\sin\theta\,\frac{dP_\tau^m}{d\theta}\right) = \left[-\tau'(\tau'+1)\sin\theta + \frac{m^2}{\sin\theta}\right]P_{\tau'}^m. \qquad \text{(A-2)}$$

Multiplying (A-1) by $P_{\tau'}^m(\cos\theta)$ and (A-2) by $P_\tau^m(\cos\theta)$ and then subtracting the second from the first, one obtains

$$[\tau'(\tau'+1)-\tau(\tau+1)]\sin\theta\;P_\tau^m P_{\tau'}^m = \frac{d}{d\theta}\left[\sin\theta\left(P_{\tau'}^m\frac{dP_\tau^m}{d\theta} - P_\tau^m\frac{dP_{\tau'}^m}{d\theta}\right)\right] \qquad \text{(A-3)}$$

which, after integrating from θ_1 to θ_2, becomes

$$[\tau'(\tau'+1)-\tau(\tau+1)]\int_{\theta_1}^{\theta_2}\sin\theta\;P_\tau^m P_{\tau'}^m d\theta = \sin\theta\left[P_{\tau'}^m\frac{dP_\tau^m}{d\theta} - P_\tau^m\frac{dP_{\tau'}^m}{d\theta}\right]\Bigg|_{\theta_1}^{\theta_2}. \qquad \text{(A-4)}$$

If we now add and subtract $k'P_\tau^m P_{\tau'}^m$ from the right side of this equation, where k' is a constant, it may be expressed thus:

$$\sin\theta\left[P_{\tau'}^m\left\{\frac{dP_\tau^m}{d\theta} + k'P_\tau^m\right\} - P_\tau^m\left\{\frac{dP_{\tau'}^m}{d\theta} + k'P_{\tau'}^m\right\}\right]\Bigg|_{\theta_1}^{\theta_2}. \qquad \text{(A-5)}$$

It is thus evident that if the τ's are distinct roots of the equation,

$$\frac{dP_\tau^m}{d\theta} + k'P_\tau^m(\cos\theta) = 0, \qquad \text{(A-6)}$$

at each of the limits, θ_1 and θ_2, then the functions are orthogonal. It may be further noted that the value of k' may be different at the two limits (Ref. 22, p. 431).

Using an analogous procedure for the equation for the spherical Hankel functions,

$$\frac{d}{d\rho}\left[\rho^2\left(\frac{dh_\tau}{d\rho}\right)\right] = [\tau(\tau+1)-\rho^2]\,h_\tau, \qquad \text{(A-7)}$$

one obtains

$$[\tau'(\tau'+1)-\tau(\tau+1)]\int_e^f h_{\tau'}h_\tau d\rho = \rho^2\left[\, h_\tau \frac{dh_{\tau'}}{d\rho} - h_{\tau'}\frac{dh_\tau}{d\rho}\,\right]\Bigg|_e^f, \qquad \text{(A-8)}$$

and finds that the Hankel functions will be orthogonal between two arbitrary limits, $\rho = e, f$, if at each limit the equation,

$$\frac{dh_\tau}{d\rho} + k''h_\tau = 0, \qquad \text{(A-9)}$$

is satisfied.

By referring to figure 3, it may be seen that the appropriate limits to use for the finite cone are $\theta = 0, \theta_0$, and $r = b, \infty$ ($\rho = kr$). For $\theta = 0$ and $r = \infty$, however, the expressions on the right-hand sides of equations (A-4) and (A-8) are zero, and equations (A-6) and (A-9) need to be considered only for $\theta = \theta_0$, $r = b$, respectively.

Let us further choose $k' = k''$, and then let k' and τ be the simultaneous solution of the equations

$$\left.\frac{dP_\tau^1}{d\theta}\right|_{\theta=\theta_0} + k'P_\tau^1(\cos\theta_0) = 0, \qquad \text{(A-10)}$$

$$\left.\frac{dh_\tau}{d\rho}\right|_{\rho=kb} + k'h_\tau(kb) = 0. \qquad \text{(A-11)}$$

Then τ must be a root of the equation,

$$\left.\frac{dP_\tau^1}{d\theta}\right|_{\theta=\theta_0} - \frac{P_\tau^1(\cos\theta_0)}{h_\tau(kb)}\left.\frac{dh_\tau}{d\rho}\right|_{\rho=kb} = 0, \qquad \text{(A-12)}$$

and thus the function $h_\tau(kr)P_\tau^m(\cos\theta)$ would be orthogonal between both sets of limits, $r = b, \infty$; $\theta = 0, \theta_0$. This procedure thus provides orthogonal integrations when matching the fields across the imaginary spherical and conical boundaries indicated in figure 3.

For such an attack on the problem, one could then choose for the function Φ in equation (2),

$$j_\tau(kr)P_\tau^1(\cos\theta)\begin{bmatrix}\sin\phi\\ \cos\phi\end{bmatrix} \quad \text{in region I,}$$

$$h_\tau(kr)P_\tau^1(\cos\theta)\begin{bmatrix}\sin\phi\\ \cos\phi\end{bmatrix} \quad \text{in region II,}$$

$$h_\tau(kr)P_\tau^1(-\cos\theta)\begin{bmatrix}\sin\phi\\ \cos\phi\end{bmatrix} \quad \text{in region III.}$$

The foregoing method of approach to the solution of the problem, though perhaps providing the finality of the coefficients, raises other problems which cause additional difficulty. In each region, field expansions must be obtained for the incident wave in terms of the non-integral degree Legendre functions, and since the value of the degree has been determined, it can no longer be chosen so as to satisfy the boundary condition at the surface of the cone, as was done in the present solution. Furthermore, the determination of the roots of equation (A-12), if they do exist, presents a problem in itself. In addition, the equation is complex and one may then expect complex roots, which, in turn, lead to resultant difficulties in determining the Bessel, Hankel, and associated Legendre functions. For these reasons, the method used in this paper was that in which the expansion coefficients do not possess finality, but appear in an infinite set of equations.

APPENDIX B

FIELD SINGULARITIES

A. Sharp Edges

Consider the electromagnetic fields which may possibly exist in the vicinity of a sharp edge. Since, for the time harmonic case, Maxwell's equations become

$$\text{curl } \bar{E} = -i\omega\mu\bar{H}, \qquad \text{curl } \bar{H} = +i\omega\epsilon\bar{E}, \tag{B-1}$$

and since the vector functions listed in equation (3) are related in this manner:

$$\text{curl } \bar{m} = k\bar{n}, \qquad \text{curl } \bar{n} = k\bar{m}, \tag{B-2}$$

where $k = 2\pi/\lambda$, these vector functions may be used to represent the electromagnetic field quantities. Furthermore, if we assume that they form a complete set of functions, then we may represent any time-harmonic electromagnetic field by an appropriate sum. For the illustration shown in figure 7, these functions become

$$\bar{m}_{\substack{e\\o}\upsilon\xi} = \mp \frac{\upsilon}{\rho} Z_\upsilon(\xi\rho) \begin{matrix}\sin\\\cos\end{matrix} \upsilon\theta\bar{a}_\rho - \frac{d}{d\rho} Z_\upsilon(\xi\rho) \begin{matrix}\cos\\\sin\end{matrix} \upsilon\theta\bar{a}_\theta, \tag{B-3}$$

$$\bar{n}_{\substack{e\\o}\upsilon\xi} = \frac{ih}{k} \frac{d}{d\rho} Z_\upsilon(\xi\rho) \begin{matrix}\cos\\\sin\end{matrix} \upsilon\theta\bar{a}_\rho \mp \frac{ih\upsilon}{k\rho} Z_\upsilon(\xi\rho) \begin{matrix}\sin\\\cos\end{matrix} \upsilon\theta\bar{a}_\theta + \frac{\xi^2}{k} Z_\upsilon(\xi\rho) \begin{matrix}\cos\\\sin\end{matrix} \upsilon\theta\bar{a}_z, \tag{B-4}$$

where h is the wave constant for the z-direction [i.e., $e^{i(\omega t - hz)}$], ξ is the wave constant for the radial direction, $Z_\upsilon(\xi\rho)$ is a cylindrical Bessel function of any kind, and $\bar{a}_\rho$, $\bar{a}_\theta$, and $\bar{a}_z$ are unit vectors.

SHARP EDGE

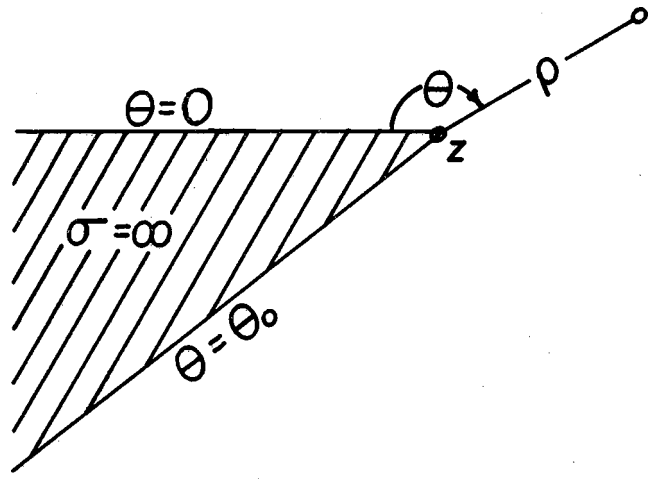

Figure 7

SHARP TIP

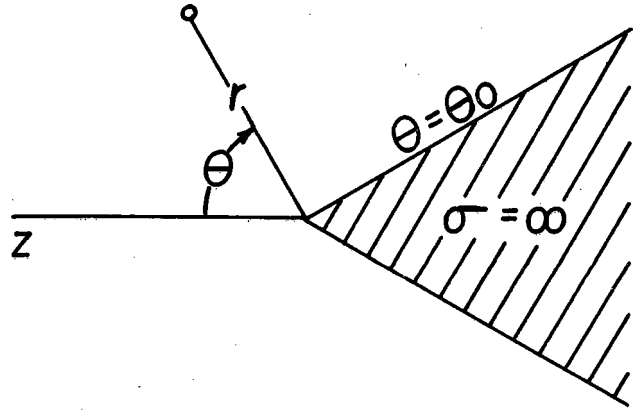

Figure 8

In cylindrical coordinates, the finite energy condition becomes

$$\int (\epsilon_o E^2 + \mu_o H^2) dV = \int (\epsilon_o E^2 + \mu_o H^2) \rho d\rho d\theta dz \rightarrow \text{finite}, \tag{B-5}$$

and thus the fields may possess at most a singularity of order $\rho^{\mu-1}$ where $\mu > 0$. Thus, in using (B-3) or (B-4) to represent the fields, one observes that υ must always be positive, since the first term in the series expansions of $\frac{Z_\upsilon(\xi\rho)}{\rho}$ and $\frac{dZ_\upsilon(\xi\rho)}{d\rho}$ vary as $\rho^{(\upsilon-1)}$.

If we assume that the wedge is perfectly conducting, then $E_\rho = E_z = H_\theta = 0$ at $\theta = 0, \theta_o$. If we first let $\bar{E}$ be represented by $\bar{m}_e$ (here we must choose the even function due to the θ variation), then $\bar{H}$ will be represented by $\bar{n}_e$. The boundary conditions are then satisfied by

$$\sin \upsilon\theta_o = 0, \quad \upsilon\theta_o = n\pi,$$

where n is zero or an integer. Since we are particularly interested in the case for $\upsilon < 1$, this only occurs for $n = 1$,

$$\upsilon = \frac{\pi}{\theta_o} < 1. \tag{B-6}$$

Referring to (B-3) and (B-4) we see then that E_ρ, E_θ, H_ρ, and H_θ may be singular of order $\rho^{(\pi/\theta_o)-1}$.

Again, if we let $\bar{E}$ be represented by $\bar{n}_o$ and $\bar{H}$ by $\bar{m}_o$, we arrive at precisely the same conclusion. These results precisely agree with those of Meixner[26], who used a power series expansion for the field components.

Furthermore, the above results seem physically reasonable since a series of point charges flowing along the edge constitute a finite current in an infinitesimal volume, or an infinite current density, which is,

of course, integrable.

B. Sharp Tips

Although the conclusions for a conical tip are not as well defined as those for the wedge, a few interesting results may be observed. Let us apply the same reasoning to a conical tip in spherical coordinates. Here the finite energy condition becomes

$$\int (\epsilon_o E^2 + \mu_o H^2) dV = \int (\epsilon_o E^2 + \mu_o H^2)\, r^2 \sin\theta \; dr\, d\theta\, d\phi \rightarrow \text{finite}, \tag{B-7}$$

thus permitting singluarities of order $r^{(\mu-3/2)}$ where $\mu > 0$. For convenience, we repeat the $\bar{m}$ and $\bar{n}$ functions

$$\bar{m}_{\substack{e\\o}mv} = \mp \frac{m}{\sin\theta} z_v(kr) P_v^m(\cos\theta) \begin{matrix}\sin\\ \cos\end{matrix} m\phi \bar{a}_\theta - z_v(kr) \frac{dP_v^m}{d\theta} \begin{matrix}\cos\\ \sin\end{matrix} m\phi \bar{a}_\phi, \tag{B-8}$$

$$\bar{n}_{\substack{e\\o}mv} = \frac{v(v+1)}{kr} z_v(kr) P_v^m(\cos\theta) \begin{matrix}\cos\\ \sin\end{matrix} m\phi \bar{a}_r + z_v'(kr) \frac{dP_v}{d\theta} \begin{matrix}\cos\\ \sin\end{matrix} m\phi \bar{a}_\theta \tag{B-9}$$

$$\mp \frac{m}{\sin\theta} z_v'(kr) P_v^m(\cos\theta) \begin{matrix}\sin\\ \cos\end{matrix} m\phi \bar{a}_\phi,$$

and note that the leading term in $z_v(kr)/r$ and $z_v'(kr)$ is of the order r^{v-1} (See notation after equation 14).

If we let $\bar{E}$ be represented by $\bar{n}$, and $\bar{H}$ by $\bar{m}$, then the boundary conditions $E_r = E_\phi = H_\theta = 0$ at $\theta = \theta_o$ are satisfied by

$$P_v^m(\cos\theta_o) = 0, \tag{B-10}$$

where m is again integral. Due to the finite energy condition, we are interested in the values $-0.5 < v < 1$. However, equation (B-10) has no roots for $|v| \leq m$ (Ref. 24, p. 386), and consequently has roots in the region of our immediate interest only for $m = 0$. For this case, a glance at (B-8) and (B-9) reveals that singularities occur in all

components of the electric field ($\bar{n}$) but in none of the components of the magnetic field ($\bar{m}$), and in the electric field only for ϕ-independent field variations.

The foregoing result also seems physically reasonable, since the presence of a point charge at the tip of the cone would produce singular electric fields with no ϕ variation. One might reasonably expect that if a material were chosen which was assumed to contain point dipoles, a singular electric field with a $\begin{bmatrix}\cos\phi\\ \sin\phi\end{bmatrix}$ variation would result.

Left to consider, then, is the case for which $\bar{E}$ is represented by $\bar{m}$, and $\bar{H}$ by $\bar{n}$. Reference to (B-8) and (B-9) reveals that the boundary conditions $E_r = E_\phi = H_\theta = 0$ at $\theta = \theta_o$ are satisfied by

$$\left.\frac{dP_\upsilon^m(\cos\theta)}{d\theta}\right|_{\theta=\theta_o} = 0. \qquad \text{(B-11)}$$

Because of the finite energy condition, equation (B-7), and the behavior of the leading radial term, any roots of (B-11) where $-0.5 < \upsilon < 1$ will produce permissible singularities. For $-0.5 < \upsilon < 1$, however, $P_\upsilon(\cos\theta)$ is either a monotonically increasing function (for υ negative) or a monotonically decreasing function (for υ positive), and thus its first derivative possesses no zeros (except $\theta = 0$) in our immediate range of interest.

From $m = 1$, $-0.5 < \upsilon < 0$, reference to figure 11 reveals that no zeros of the first derivative occur (all values of υ in this range lie between the zero axis and the $\upsilon = -0.5$ curve plotted in figure 11). One may also observe that zeros do occur for $0.8 < \upsilon < 1$. Reference again to

(B-9) reveals singularities in all components of the magnetic field.

Since, in this case, the electric field is represented by $\bar{m}$, which possesses a leading radial term of r^{υ}, we should perhaps consider roots of (B-11) as low as -1.5 for only the electric field. Since $P_{\upsilon}^{m}(\cos\theta) = P_{-\upsilon-1}^{m}(\cos\theta)$, however, the graphs of figure 11 for $0.5 \leq \upsilon \leq -0.5$ may be also interpreted as those for $-1.5 \leq \upsilon \leq -0.5$, respectively, and no additional zeros occur.

Here again, singular magnetic field components seem reasonable, since a finite surface current flows over an infinitesimal area at the tip of the cone, producing a singularity of current density. One may further observe from figure 9 that this current would produce a singular magnetic field in the y-direction, producing the resulting singularities in all of the spherical components.

In summary, we have found that:

(a) at a perfectly conducting sharp edge, singularities of order $\frac{\pi}{\theta_o} - 1$ may occur in all components of the electric and magnetic fields except those tangential to the edge;

(b) at a perfectly conducting sharp tip, a singularity may occur in the electric field for only Φ-independent fields;

(c) at a perfectly conducting sharp tip, a singularity may occur in the magnetic field if it possesses a $\begin{bmatrix}\cos\Phi \\ \sin\Phi\end{bmatrix}$ dependence. A singularity will not occur in the magnetic field if it is Φ independent.

SURFACE CURRENTS AT A CONICAL TIP

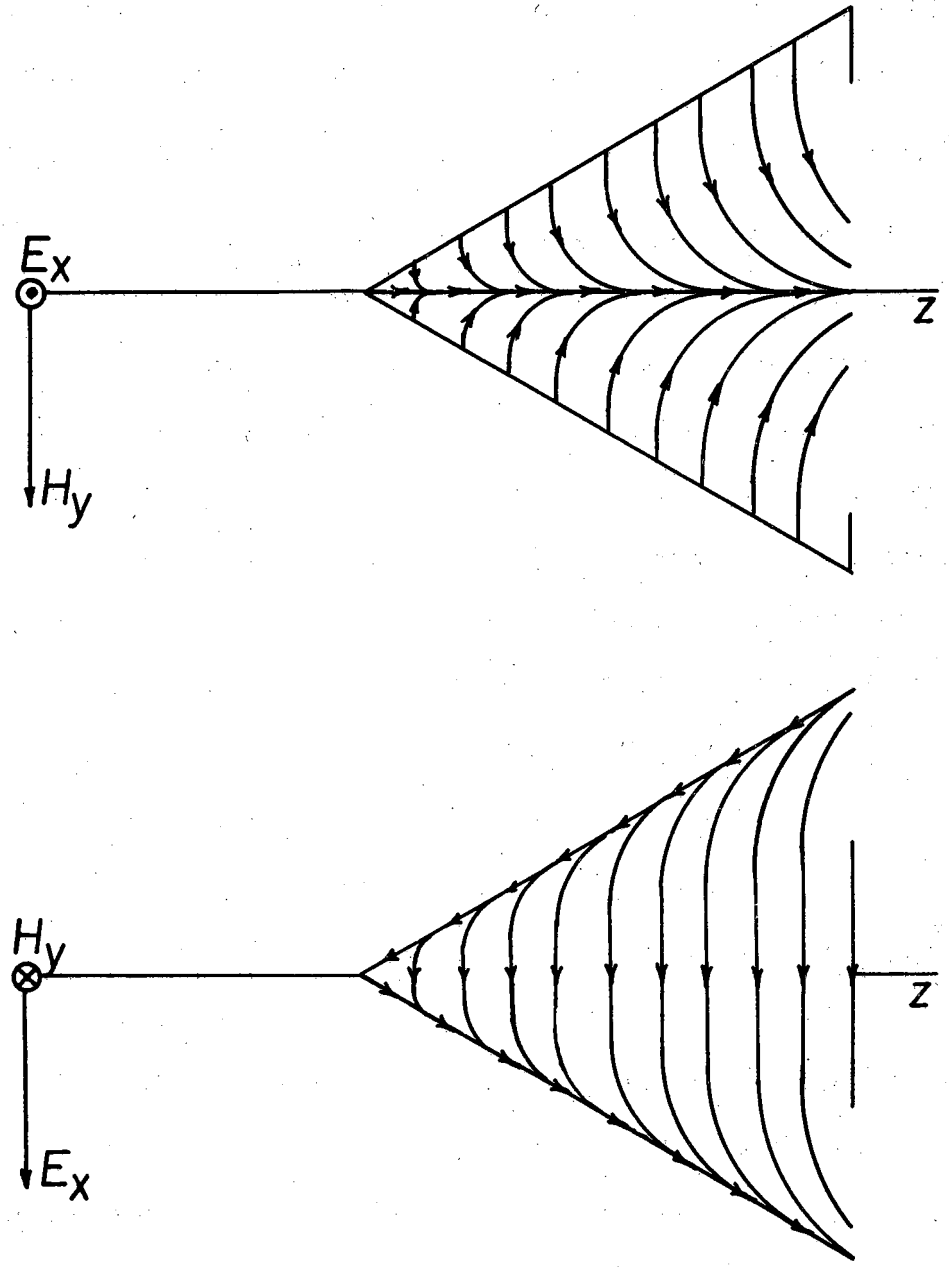

Figure 9

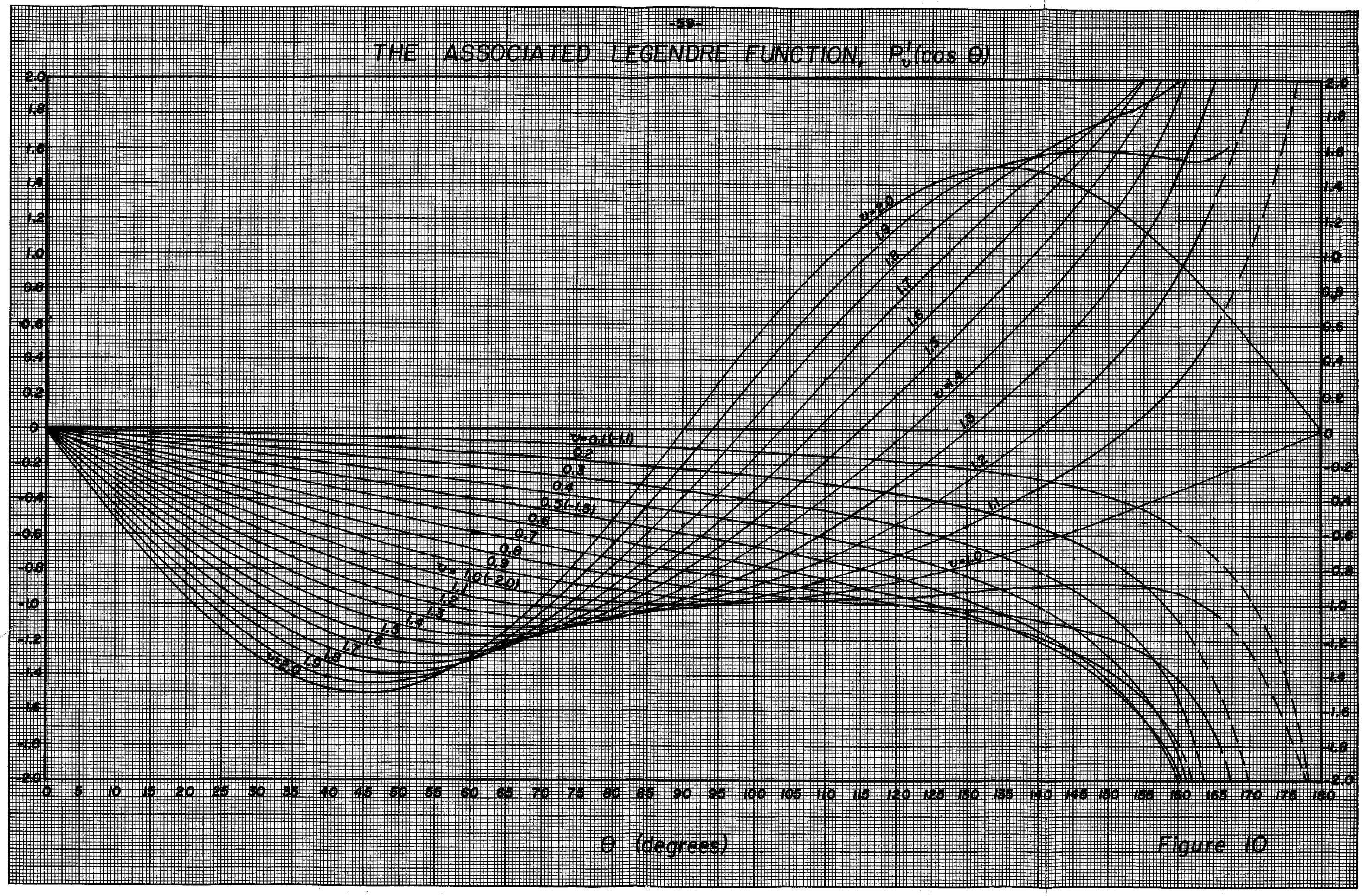
THE ASSOCIATED LEGENDRE FUNCTION, $P_\nu^1(\cos\theta)$
2.0
1.8
1.6
1.4
1.2
1.0
0.8
0.6
0.4
0.2
0
-0.2
-0.4
-0.6
-0.8
-1.0
-1.2
-1.4
-1.6
-1.8
-2.0
0 5 10 15 20 25 30 35 40 45 50 55 60 65 70 75 80 85 90 95 100 105 110 115 120 125 130 135 140 145 150 155 160 165 170 175 180
θ (degrees)
ν=0.1(.1).0
ν=1.0
ν=1.01(.01)1.09
ν=1.1(.1)2.0

Figure 10

THE FIRST DERIVATIVE OF THE ASSOCIATED LEGENDRE FUNCTION, $\frac{dP_\nu^1(\cos\theta)}{d\theta}$

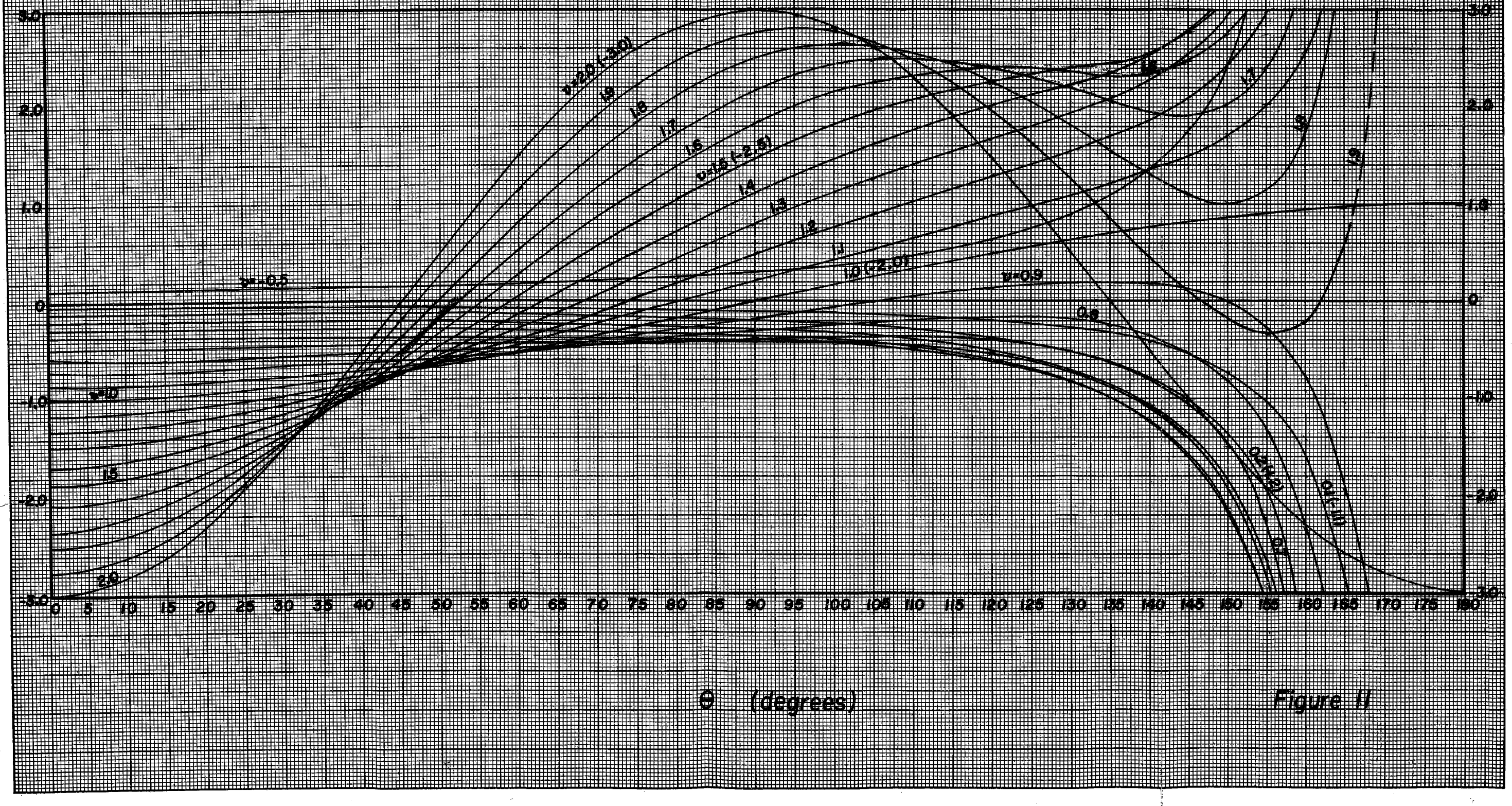

Figure II

APPENDIX C

A NOTE ON THE COMPUTATION OF THE ASSOCIATED LEGENDRE FUNCTION

In order to compute the associated Legendre functions to a desired degree of accuracy, the hypergeometric series, equation (75), was used:

$$F(\alpha,\beta;\gamma;z) = 1 + \frac{\alpha\beta}{\gamma 1!} z + \frac{\alpha(\alpha+1)\beta(\beta+1)}{\gamma(\gamma+1)2!} z^2 + \cdots .$$

For the associated Legendre function, we have

$$\begin{aligned} \alpha &= m-\upsilon \\ \beta &= m+\upsilon+1 \\ \gamma &= m+1 \\ z &= \frac{1-\cos\theta}{2}, \end{aligned} \tag{C-1}$$

and since z is always positive and less than unity, the magnitude of the ratio of the succeeding terms will be less than unity if

$$\frac{(\alpha+N)(\beta+N)}{(\gamma+N)(N+1)} < 1 \tag{C-2}$$

For $P_\upsilon^1(\cos\theta)$, it may easily be shown that (C-2) is satisfied for any N if υ is positive, and if υ is negative one must have

$$(N+1)(N+2) > \frac{\upsilon(\upsilon+1)}{2} . \tag{C-3}$$

Thus, if N satisfies (C-3), an upper limit on the remainder of the series after N terms may be obtained by assuming each term to have the coefficient of the Nth term. Thus, if

$$F(\alpha,\beta;\gamma,z) = 1 + \frac{\alpha\beta}{\gamma 1!} z + \cdots + \frac{\alpha\cdots(\alpha+N)\beta\cdots(\beta+N)}{\gamma\cdots(\gamma+N)(N+1)!} z^N + R(N), \tag{C-4}$$

where R(N) is the remainder, then

$$R(N) < \frac{\alpha\cdots(\alpha+N)\beta\cdots(\beta+N)}{\gamma\cdots(\gamma+N)(N+1)!} \sum_{n=N+1}^{\infty} z^n$$

$$= \frac{\alpha\cdots(\alpha+N)\beta\cdots(\beta+N)}{\gamma\cdots(\gamma+N)(N+1)!} z^{N+1} \sum_{n=0}^{\infty} z^n \qquad (C\text{-}5)$$

$$= \frac{\alpha\cdots(\alpha+N)\beta\cdots(B+N)}{\gamma\cdots(\gamma+N)(N+1)!} z^N \left[\frac{z}{1-z}\right].$$

Thus, by multiplying the last computed term of the series by $\frac{z}{1-z}$, one may be certain of the accuracy obtained.

Using this procedure, tables were computed, accurate to six decimal places, for the following associated Legendre functions:

$$P_\upsilon^1(\cos\theta) \begin{bmatrix} \theta \rightarrow (5°[5°]165°) \\ \upsilon \rightarrow (-0.5[0.1]3.0) \end{bmatrix}$$

$$\frac{dP_\upsilon^1(\cos\theta)}{d\theta} \begin{bmatrix} \theta \rightarrow (5°[5°]165°) \\ \upsilon \rightarrow (-0.5[0.1]2.0) \end{bmatrix}$$

Utilizing the relation $P^m_{-\upsilon-1} = P^m_\upsilon$, the range of υ may be further extended.

All computations included in this report were performed on the Burroughs Datatron 205. Total time required was approximately sixteen hours, including computation of the tables cited above.

It is anticipated that more computations will be made on the determination of the roots of equations (32) and (34), as well as for the corresponding spherical Bessel functions, thus enabling theoretical determination of the radar cross sections of finite cones in the resonance region.

DISTRIBUTION LIST

Code	Organization	* No. of Copies
AF 15	ARDC (RDSPE-3) Andrews AFB, Wash 25, D. C.	
AF 29	APGC (PGTRI, Tech Lib) Eglin AFB, Fla.	
AF 69	Director of Resident Training 3380th Technical Training Group Keesler AFB, Mississippi Attn: OA-3011 Course	
AF 18	AUL Maxwell AFB, Ala.	
AF 5	AF Missile Test Cen Patrick AFB, Fla. Attn: AFMTC, Tech Library, MU-135	
AF 91	AFOSR (SRY, Mr. Otting) 14th Street and Constitution Avenue Washington, D. C.	
AF 166	Hq USAF (AFOAC-S/E) Communications-Electronics Directorate Wash 25, D. C.	
AF 63	WADD (WCLRSA, Mr. Portune) Wright-Patterson AFB, Ohio	
AF 68	WADD (WCLRE-5) Attn: Mr. Paul Springer Wright-Patterson AFB, Ohio	
AF 231	Director, Electronics Division Air Technical Intelligence Center Attn: AFCIN-4E1, Colonel H. K. Gilbert Wright-Patterson AFB, Ohio	
AF 120	RADC (RCUE) Attn: Mr. Donald Dakan Griffiss AFB, N. Y.	
AF 139	AF Missile Dev. Cen. (MDGRT) Attn; Technical Library Holloman AFB, New Mexico	

*Note: One copy unless otherwise designated.

Code	Organization	No. of Copies
AF 308	WADD (WWDRTR, Mr. A. D. Clark) Directorate of System Engineering Dyna Soar Engineering Office Wright-Patterson AFB, Ohio	
Ar 47	Ballistic Research Laboratories Aberdeen Proving Ground, Maryland Attn: Technical Information Branch	
Ar 5	U. S. Army Signal Engineering Laboratories Evans Signal Laboratory Belmar, New Jersey Attn: Technical Document Center	
Ar 10	Massachusetts Institute of Technology Signal Corps Liaison Officer Cambridge 39, Mass. Attn: A. D. Bedrosian, Room 26-131	
Ar 67	Commander Army Rocket & Guided Missile Agency Redstone Arsenal, Alabama Attn: Technical Library, ORDXR-OTL	2
Ar 9	Department of the Army Office of the Chief Signal Officer Washington 25, D. C. Attn: Research & Development Division, OCSigO	
Ar 41	Office of Chief Signal Officer Engineering & Technical Division Washington 25, D. C. Attn: SIGNET-5	
Ar 48	Guided Missile Fuze Library Diamond Ordnance Fuze Laboratories Washington 25, D. C. Attn: R. D. Hatcher, Chief Microwave Development Section	
G 2	ASTIA Arlington Hall Station Arlington 12, Virginia	10

Code	Organization	No. of Copies
G 8	Library Boulder Laboratories National Bureau of Standards Boulder, Colorado	
G 27	National Bureau of Standards U. S. Department of Commerce Washington 25, D. C. Attn: Gustave Shapiro, Chief Engineering Electronics Section Electricity and Electronics Division	
G 6	Office of Technical Services Department of Commerce Washington 25, D. C. Attn: Technical Reports Section	2
G 103	National Aeronautical Space Agency Langley Aeronautical Research Laboratory Langley, Virginia Attn: Mr. Cliff Nelson	
M 6	AFCRL AFRD (CRREL-4) L. G. Hanscom Field, Bedford, Mass.	10
M 17	AFCRL AFRD (CRRD) Attn: Carlyle J. Sletten L. G. Hanscom Field, Bedford, Mass.	3
	AFCRL AFRD (CRRD) Attn: Contract Files L. G. Hanscom Field, Bedford, Mass.	2
N 3	Chief, Bureau of Ships Department of the Navy Washington 25, D. C. Attn: Code 690	
N 23	U. S. Naval Ordnance Laboratory White Oak, Silver Spring 19, Maryland Attn: The Library	
N 27	Librarian U. S. Naval Postgraduate School Monterey, California	

Code	Organization	No. of Copies
N 30	Dr. J. I. Bohnert, Code 5210 U. S. Naval Research Laboratory Washington 25, D. C.	
N 35	Commanding Officer and Director U. S. Navy Underwater Sound Laboratory Fort Trumbull, New London, Connecticut	
N 37	Chief of Naval Research Department of the Navy Washington 25, D. C. Attn: Code 427	
N 139	Commanding Officer and Director U. S. Navy Electronics Laboratory San Diego 52, California Attn: Code 2420 - 1 copy Attn: Code 2744 - 1 copy	
N 9	Chief, Bureau of Ordnance Department of the Navy Washington 25, D. C. Attn: Code Ad3	
N 86	Chief, Bureau of Ordnance Department of the Navy Surface Guided Missile Branch Washington 25, D. C. Attn: Code RdS1-e	
N 88	Department of the Navy Bureau of Aeronautics Technical Data Division, Code 4106 Washington 25, D. C.	
N 48	Commanding Officer U. S. Naval Air Development Center Johnsville, Pennsylvania Attn: NADC library	
N 141	ARDC Regional Office c/o Department of the Navy Room 4549, Munitions Building, Wash 25, D. C.	

Code	Organization	No. of Copies
N 93	Commanding Officer U. S. Naval Ordnance Laboratory Corona, California Attn: Documents Librarian	
I 601	Aero Geo Astro Corp. 1914 Duke Street Alexandria, Virginia Attn: George G. Chadwick	
I 1	Airborne Instruments Laboratory, Inc. Division of Cutler Hammer Walt Whitman Road, Melville, L. I. New York Attn: Dr. E. G. Fubine Director, Res. and Eng. Division	
I 205	Battelle Memorial Institute 505 King Avenue Columbus 1, Ohio Attn: Wayne E. Rife, Project Leader Electrical Engineering Division	
I 8	Bell Aircraft Corporation Post Office Box One Buffalo 5, New York Attn: Eunice P. Hazelton, Librarian	
I 13	Bell Telephone Laboratories, Inc. Whippany Laboratory Whippany, New Jersey Attn: Technical Information Library	
I 246	Bendix Aviation Corporation Pacific Division 11600 Sherman Way North Hollywood, California Attn: Engineering Library	
I 247	Bendix Radio Division Bendix Aviation Corporation E. Joppa Road Towson 4, Maryland Attn: Dr. D. M. Allison, Jr. Director Engineering & Research	

Code	Organization	No. of Copies
I 469	Bell Telephone Laboratories Murray Hill New Jersey	
I 892	Boeing Aircraft Company Seattle 15, Washington Attn: Mr. D. Scidmore	
I 254	Convair, A Division of General Dynamics Corp. 3165 Pacific Highway San Diego 12, California Attn: Mrs. Dora B. Burke, Engineering Librarian	
I 25	Cornell Aeronautical Laboratory, Inc. 4455 Genesee Street Buffalo 21, New York Attn: Librarian	
I 255	Dalmo Victor Company A Division of Textron, Inc. 1515 Industrial Way Belmont, California Attn: Mary Ellen Addems, Technical Librarian	
I 28	Dorne and Margolin, Inc. 29 New York Avenue Westbury, Long Island, N. Y.	
I 257	Douglas Aircraft Co., Inc. 827 Lapham Street El Segundo, California Attn: Engineering Library	
I 258	Douglas Aircraft Company, Inc. 3000 Ocean Park Boulevard Santa Monica, California Attn: Peter Duyan, Jr. Chief, Electrical/Electronics Section	
I 259	Douglas Aircraft Company, Inc. 2000 North Memorial Drive Tulsa, Oklahoma Attn: Engineering Librarian, D-250	

Code	Organization	No. of Copies
I 187	Electromagnetic Research Corporation 711-14th Street, N. W. Washington 5, D. C.	
I 415	Electronics Communication 1830 York Road Timonium, Maryland	
I 264	Fairchild Aircraft-Missiles Division Fairchild Eng. and Airplane Corp. Hagerstown, Maryland Attn: Library	
I 266	Federal Telecommunication Laboratories 500 Washington Avenue Nutley 10, New Jersey Attn: Technical Library	
I 269	General Electric Company Electronics Park Syracuse, New York Attn: Documents Library B. Fletcher, Building 3-143A	
I 270	General Precision Laboratory, Inc. 63 Bedford Road Pleasantville, New York Attn: Librarian	
I 48	Goodyear Aircraft Corp. 1210 Massillon Road Akron 15, Ohio Attn: Library, Plant G	
I 448	Granger Associates Electronic Systems 974 Commercial Street Palo Alto, California Attn: John V. N. Granger, President	
I 272	Grumman Aircraft Engineering Corporation Bethpage, Long Island, New York Attn: Engineering Librarian, Plant No. 5	

Code	Organization	No. of Copies
I 793	General Electric Company Missile and Space Vehicle Department 3198 Chestnut Street, Philadelphia, Pennsylvania Attn: Documents Library	
I 893	General Electric Company 3750 D Street Philadelphia 24, Pa. Attn: Mr. H. G. Lew Missile and Space Vehicle Department	
I 207	Hughes Aircraft Company Antenna Department Building 12, Mail Station 2617 Culver City, California Attn: Dr. W. H. Kummer	
I 56	Hughes Aircraft Company Florence and Teale Streets Culver City, California Attn: Dr. L. C. Van Atta, Associate Director Research Laboratories	
I 230	Jansky and Bailey, Inc. 1339 Wisconsin Avenue, N. W. Washington 7, D. C. Attn: Mr. Delmer C. Ports	
I 468	Lockheed Aircraft Corporation Missile Systems Division Research Library Box 504, Sunnyvale, California Attn: Miss Eva Lou Robertson, Chief Librarian	
I 136	The Martin Company P. O. Box 179 Denver 1, Colorado Attn: Mr. Jack McCornick	
I 280	The Martin Company Baltimore 3, Maryland Attn: Engineering Library Antenna Design Group	
I 63	Mathematical Reviews 190 Hope Street Providence 6, Rhode Island	

Code	Organization	No. of Copies
I 282	McDonnell Aircraft Corporation Lambert-Saint-Louis Municipal Airport Box 516, St. Louis 3, Missouri Attn: R. D. Detrich, Engineering Library	
I 116	Melpar, Inc. 3000 Arlington Boulevard Falls Church, Virginia Attn: Engineering Technical Library	
I 641	National Research Council Radio & Electrical Engineering Division Ottawa, Ontario, Canada Attn: Dr. G. A. Miller, Head Microwave Section	
I 284	North American Aviation, Inc. 12214 Lakewood Boulevard Downey, California Attn: Engineering Library 495-115	
I 285	North American Aviation, Inc. Los Angeles International Airport Los Angeles 45, California Attn: Engineering Technical File	
I 232	Radiation Engineering Laboratory Main Street Maynard, Mass. Attn: Dr. John Ruze	
I 289	Radiation, Inc. P. O. Drawer 37 Melbourne, Florida Attn: Technical Library, Mr. M. L. Cox	
I 233	Radio Corporation of America RCA Laboratories Rocky Point, New York Attn: P. S. Carter, Lab. Library	
I 290	RCA Laboratories David Sarnoff Research Center Princeton, New Jersey Attn: Miss Fern Cloak, Librarian	

Code	Organization	No. of Copies
I 291	Radio Corporation of America Defense Electronic Products Building 10, Floor 7 Camden 2, New Jersey Attn: Mr. Harold J. Schrader, Staff Engineer Organization of Chief Technical Administrator	
I 473	Radio Corporation of America Aviation Systems Laboratory 225 Crescent Street Waltham, Mass.	
I 757	Radio Corporation of America Surface Communications Systems Laboratory 75 Varick Street, New York 13, N. Y. Attn: Mr. S. Krevsky	
I 789	Radio Corporation of America West Coast Missile and Surface Radar Division Engineering Library, Building 306/2 Attn: L. R. Hund, Librarian 8500 Balboa Boulevard, Van Nuys, California	
I 292	Director USAF Project RAND via: AF Liaison Office The Rand Corporation 1700 Main Street Santa Monica, California	
I 294	Raytheon Company Wayland Laboratory Wayland, Mass. Attn: Miss Alice G. Anderson, Librarian	
I 472	Raytheon Company Missile Systems Division Hartwell Road, Bedford, Mass. Attn: Donald H. Archer	
I 96	Sandia Corporation, Sandia Base P. O. Box 5800, Albuquerque, New Mexico Attn: Classified Document Division	

Code	Organization	No. of Copies
I 312	Space Technology Laboratories, Inc. P. O. Box 95001 Los Angeles 45, California Attn: Mrs. Margaret C. Whitnah Chief, Information Services	2
I 367	Stanford Research Institute Documents Center Menlo Park, California Attn: Acquisitions	
I 104	Sylvania Electric Products, Inc. 100 First Avenue, Waltham 54, Mass. Attn: Charles A. Thornhill, Report Librarian Waltham Laboratories Library	
I 818	Sylvania Reconnaissance Systems Lab. Box 188, Mountain View, California Attn: Marvin D. Waldman	
I 260	Sylvania Elec. Prod. Inc. Electronic Defense Laforatory P. O. Box 205 Mountain View, California Attn: Library	
U 61	Brown University Department of Electrical Engineering Providence, Rhode Island Attn: Dr. C. M. Angulo	
U 99	California Institute of Technology 1201 E. California Street Pasadena, California Attn: Dr. C. Papas	
U 3	Space Sciences Laboratory Leuschner Observatory University of California Berkeley 4, California Attn: Dr. Samuel Silver, Professor of Engineering Science and Director, Space Sciences Laboratory	
U 100	University of California Electronics Research Lab. 332 Cory Hall, Berkeley 4, California Attn: J. R. Whinnery	

Code	Organization	No. of Copies
U 289	University of Southern California University Park Los Angeles California Attn: Dr. Raymond L. Chuan Director, Engineering	
U 182	Case Institute of Technology 10900 Euclid Avenue Cleveland, Ohio Attn: Prof. S. Seeley	
U 183	Columbia University Department of Electrical Engineering Morningside Heights New York, N. Y. Attn: Dr. Schlesinger	
U 238	University of Southern California University Park Los Angeles 7, California Attn: Z. A. Kaprielian Associate Professor of Electrical Engineering	
U 10	Cornell University School of Electrical Engineering Ithaca New York Attn: Prof. G. C Dalman	
U 59	Library Georgia Technology Research Institute Engineering Experiment Station, 722 Cherry Street, N. W. Atlanta, Georgia Attn: Mrs. J. H. Crosland, Librarian	
U 102	Harvard University Technical Reports Collection Gordon McKay Library 303 Pierce Hall Oxford Street, Cambridge 38, Mass. Attn: Librarian	
U 103	University of Illinois Documents Division Library Urbana, Illinois	

Code	Organization	No. of Copies
U 240	Illinois Institute of Technology Technology Center Department of Electrical Engineering Chicago 16, Illinois Attn: Paul C. Yuen Electronics Research Laboratory	
U 22	The Johns Hopkins University Homewood Campus Baltimore 18, Maryland Attn: Dr. Donald E. Kerr Dept. of Physics	
U 228	University of Kansas Electrical Engineering Department Lawrence, Kansas Attn: Dr. H. Unz	
U 68	Lowell Technological Institute Research Foundation P. O. Box 709, Lowell, Mass. Attn: Dr. Charles R. Mingins	
U 32	Massachusetts Institute of Technology Research Laboratory of Electronics Building 26, Room 327 Cambridge 39, Mass. Attn: John H. Hewitt	
U 26	Massachusetts Institute of Technology Lincoln Laboratory P. O. Box 73 Lexington 73, Mass. Attn: Mary A. Granese, Librarian	
U 34	McGill University Montreal, Canada Attn: Prof. G. A. Woonton Director, The Eaton Electronics Research Laboratory	
U 79	University of Michigan Engineering Research Institute Radiation Laboratory 912 N. Main Street, Ann Arbor, Michigan Attn: Prof. K. M. Siegel	

Code	Organization	No. of Copies
U 37	University of Michigan Engineering Research Institute Willow Run Laboratories, Willow Run Airport Ypsilanti, Michigan Attn: Librarian	
U 39	New York University Institute of Mathematical Sciences Room 802, 25 Waverly Place New York 3, New York Attn: Professor Morris Kline	
U 96	Northwestern University Microwave Laboratories Evanston, Illinois Attn: R. E. Beam	
U 78	Ohio State University Research Foundation 1314 Kinnear Road Columbus 8, Ohio Attn: Dr. T. E. Tice Department of Electrical Engineering Classified to go thru: Dr. Arthur S. Cosler, Jr.	
U 45	The Pennsylvania State University Department of Electrical Engineering University Park, Pennsylvania	
U 185	University of Pennsylvania Institute of Cooperative Research 3400 Walnut Street, Philadelphia, Pa. Attn: Department of Electrical Engineering	
U 48	Polytechnic Institute of Brooklyn Microwave Research Institute 55 Johnson Street, Brooklyn New York Attn: Dr. Arthur A. Oliner	
U 176	Stanford University W. W. Hansen Laboratory of Physics Stanford, California Attn: Microwave Library	